land

MDPI

Article

Application of the Analytic Network Process for Sub-Watershed Prioritization in the Huehuetan River Basin, Chiapas, Mexico

Adolfo López-Pérez [1,*], Gerardo Colín-García [2], Héctor Moya [3], Martín Alejandro Bolaños-González [1], Demetrio Salvador Fernández-Reynoso [1] and Angel Saul Cruz-Ramírez [4]

[1] Posgrado de Hidrociencias, Colegio de Postgraduados, Campus Montecillo, Texcoco 56264, Mexico; bolanos@colpos.mx (M.A.B.-G.); demetrio@colpos.mx (D.S.F.-R.)
[2] Centro de Investigación Regional Pacifico Sur, Campo Experimental Centro de Chiapas, Instituto Nacional de Investigaciones Forestales, Agrícolas y Pecuarias (INIFAP), Ocozocoautla de Espinosa 29140, Mexico; colin.gerardo@inifap.gob.mx
[3] Centro Regional de Investigación e Innovación para la Sostenibilidad de la Agricultura y los Territorios Rurales (CERES), Pontificia Universidad Católica de Valparaíso, Quillota 2260000, Chile; hmoya@centroceres.cl
[4] Centro Nacional de Investigación Disciplinaria en Conservación y Mejoramiento de Ecosistemas Forestales, Instituto Nacional de Investigaciones Forestales, Agrícolas y Pecuarias (INIFAP), Ciudad de México 04010, Mexico; cruz.saul@inifap.gob.mx
* Correspondence: adolfholp@colpos.mx; Tel.: +521-595-110-9896

Abstract: Sub-watershed prioritization is essential for developing watershed management plans that maximize impact with minimal resources. This study used a multicriteria decision-making approach to rank sub-watersheds by degradation status in the Huehuetan River Basin, Chiapas, Mexico. The eight sub-watersheds in the basin were classified using the Analytic Network Process (ANP) model, evaluating morphometry, hydrology, hillslope stability, soil water saturation, land-use change, and socioeconomic factors. The results identified hydrology and land-use change as the most influential criteria, with weights of 20.62% and 19.82%, respectively, driven mainly by surface runoff and deforestation. Swtr 08 and Swtr 07 were identified as the highest-priority sub-watersheds, covering 24.31% of the basin area, with 55.31% of Swtr 08 classified as unstable and showing a combined high-vegetation loss of 16.46 km^2. The entire watershed showed an annual vegetation loss rate of 146 ha year^{-1}. Increasing the weighting by 50% resulted in greater variability in priority rankings, with runoff and low vegetation showing maximum global ranges of −44.33% and 30.25%, respectively, instability decreasing by 33.94%, and peak flow increasing by 18.20%. These findings emphasize the need for focused interventions in the vulnerable subwatersheds of the upper basin to manage runoff, curb deforestation, and reduce soil instability.

Keywords: degradation; environmental restoration; geographic information systems; remote sensing; multicriteria decision-making

check for updates

Citation: López-Pérez, A.; Colín-García, G.; Moya, H.; Bolaños-González, M.A.; Fernández-Reynoso, D.S.; Cruz-Ramírez, A.S. Application of the Analytic Network Process for Sub-Watershed Prioritization in the Huehuetan River Basin, Chiapas, Mexico. *Land* **2024**, *13*, 1868. https://doi.org/10.3390/land13111868

Academic Editor: Carlos Rogério Mello

Received: 24 August 2024
Revised: 1 November 2024
Accepted: 6 November 2024
Published: 8 November 2024

Copyright: © 2024 by the authors. Licensee MDPI, Basel, Switzerland. This article is an open access article distributed under the terms and conditions of the Creative Commons Attribution (CC BY) license (https://creativecommons.org/licenses/by/4.0/).

1. Introduction

The hydrographic basin is an essential planning and management unit for modeling water resources at the watershed level [1]. It corresponds to a hydrological response unit that can be used as a socioeconomic-political unit and, therefore, is suitable for planning and implementing management plans [2]. The key characteristics of a basin, such as its size, shape, relief, drainage system, soil type, land cover, and climatic conditions, are crucial for understanding its current state [3,4]. In addition, factors like the population settled in the basin and its socioeconomic activities play a significant role in assessing the previous conditions. These characteristics facilitate understanding the watershed status and identifying the most critical aspects of environmental preservation and natural resource management [5]. Additionally, analyzing each of these elements sets the ground to establish

watershed management plans and control measures to reduce the potential impacts of degradation processes [6,7], especially in tropical regions, where variations in climate and rainfall can significantly affect access to drinking water and other municipal services [8].

Multi-Criteria Decision-Making (MCDM) is a method to determine the best possible alternative from a set of options according to criteria established for solving complex problems [6]. During the past few decades, several MCDM models have been used as alternatives to prioritize activities in different planning areas [7]. These models have been applied in precision agriculture [8], climate-change strategy plans [9], wastewater treatment planning [10], water resources management [11–13], susceptibility to landslides [14], and erosion risk assessment [15]. Implementing these methodologies in watersheds, sub-watersheds, or micro-watersheds allows prioritizing activities in vulnerable areas based on tangible results, even under limited data availability or uncertain information [16]. Most research based on the Analytic Network Process (ANP) model has been carried out in project management, risk assessment, supplier selection, and product design [1,17]. However, few studies have applied the ANP model for watershed or sub-watershed prioritization [18]. Some authors have worked with one or two criteria under the Analytic Hierarchy Process (AHP) model, a method with limitations in terms of the interrelationship between criteria [19]. In addition, according to Chen et al. [20], only two countries in America (the United States and Canada) have worked with the ANP model.

The development of public policies and their application through watershed management plans seek to generate positive impacts, maximizing the benefits while minimizing the costs [11]. However, the implementation of these plans should be analyzed not only in economic terms but also considering their potential ecological and social impacts [21,22]. In addition, in recent decades, some watersheds have presented higher levels of environmental degradation issues as a result of anthropogenic activities and human-induced climate change [23]. Furthermore, addressing the entire watershed simultaneously is not recommended because sub-watersheds should be prioritized [24]. Parameters related to the hydrological response to internal watershed processes can set the foundation for setting management priorities [25]. Therefore, prioritization of sub-watersheds can correctly and effectively guide the budget, human resources, materials, equipment, and other resources to a watershed target area, seeking to maximize the impact of management plans related to the severity of the current degradation of this watershed [22].

The Huehuetan River Basin (HRB), located in Chiapas, Mexico, is characterized by rugged relief with steep slopes, high rainfall volume and intensity, and severe environmental degradation caused by the current management of natural resources [26–28]. As a result, the watershed has been continuously affected by natural disasters, such as floods in the lowlands and landslides in the highlands [29]. For this reason, the Mexican National Water Commission (CONAGUA) implemented strategies for transferring soil and water conservation technologies to the Sierra Madre de Chiapas watersheds. These strategies seek to control water erosion and increase soil infiltration and storage of moisture, thereby reducing vulnerability and risk of disasters in the watershed [30]. However, sub-watershed prioritization based on morphometry, hydrology, slope stability, soil water saturation, land-use change, and socioeconomic conditions in the watershed has not been included in the development of conservation strategies. Therefore, this study outlines a methodological approach for sub-watershed prioritization considering several criteria associated with the watershed degradation status based on the ANP model in the HRB, an area of Mexico where the watershed has been studied for more than 15 years.

2. Materials and Methods

2.1. Description of the Study Area

The study area is the Huehuetan River Basin (HRB), which covers over 319.28 km^2 (Figure 1). Its main channel is the Huehuetan River, which originates in the Sierra Madre de Chiapas and flows down to its outlet at the hydrometric station (15°05′56″ N, 92°24′02″ W) and runs across 41.96 km. The watershed was delineated using the Soil and Water

Assessment Tool (SWAT) model (version 681), and eight sub-watersheds were identified following the methodology of Pfafstetter [31].

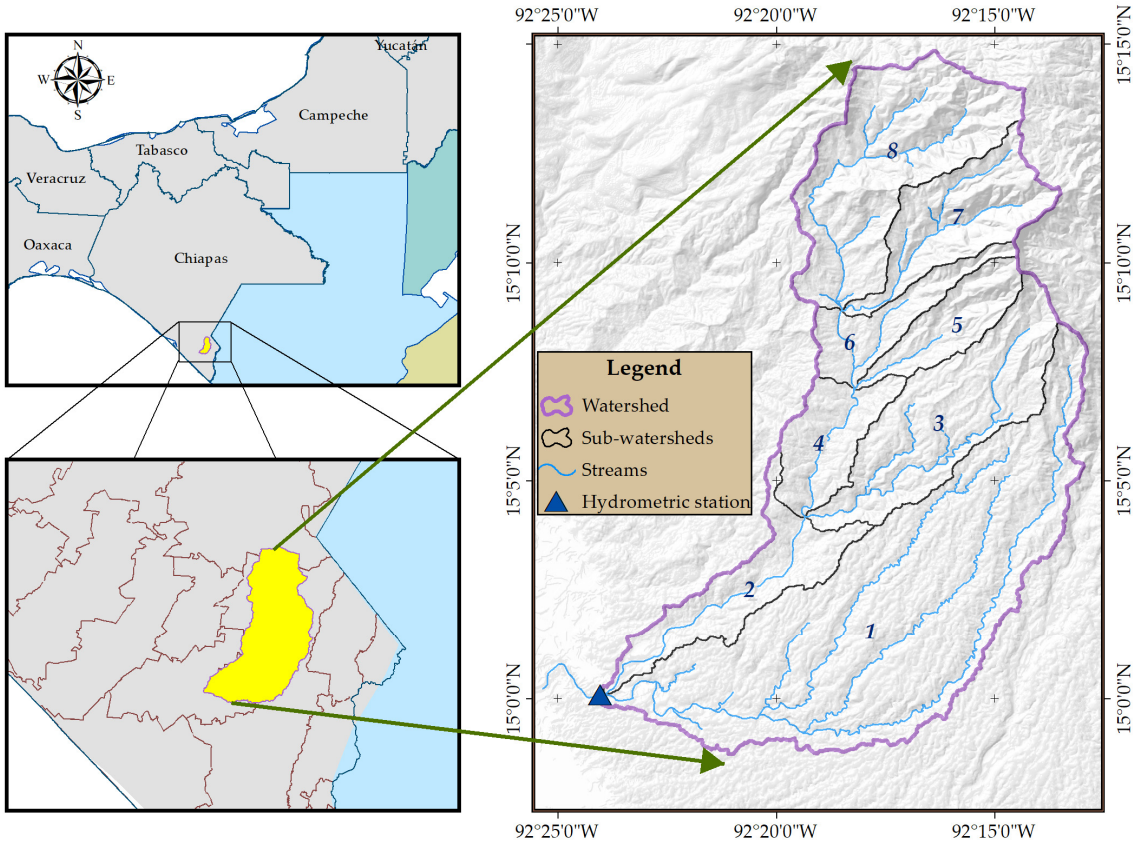

Figure 1. Location and delineation of the sub-watersheds of the Huehuetan River watershed, Chiapas, Mexico.

The HRB is characterized by a rugged terrain, especially in its middle and upper regions, with an altitudinal range between 30 m and 2690 m a.s.l. [32], and a mean altitude of 864.24 m (Figure 2a). The area has a steep mean slope of 37.88% (Figure 2b). According to Köppen's climate classification modified by García [33], warm (A) and temperate (D) climate types predominate in the watershed. The warm climate covers 83.64% of the area at altitudes below 1800 m, and the temperate climate 16.36% above 1800 m a.s.l. (Figure 2c) [34]. The geology of the watershed comprises mainly igneous (94.32%) and sedimentary (5.68%) rocks; igneous rocks include intermediate tuff, andesite, and granite, whereas sedimentary rocks consist of conglomerates and alluvial deposits, mainly in the lowlands along the Huehuetan riverbed and banks. These formations result from surface runoff, mainly in the upper region, and sediment detachment, transport, and deposition in areas with gentle slopes [35,36]. The main soil groups (Figure 2d) are Leptosols (LP, 36.79%), Andosols (AN, 28.83%), Cambisols (CM, 23.82%), and Luvisols (LV, 10.56%) [36]. Land uses in the watershed (Figure 2c) include coffee plantations (COFF, 42.40%), rainfed agriculture (TEMP, 20.37%), mountain cloud forest (FRSE, 17.58%), and mixed forest (FRST, 16.06%). The remaining area is covered by coconut palm plantations (COCT, 1.56%), grasslands (PAST, 1.16%), human settlements (URBN, 0.58%), and mango plantations (MANG, 0.29%).

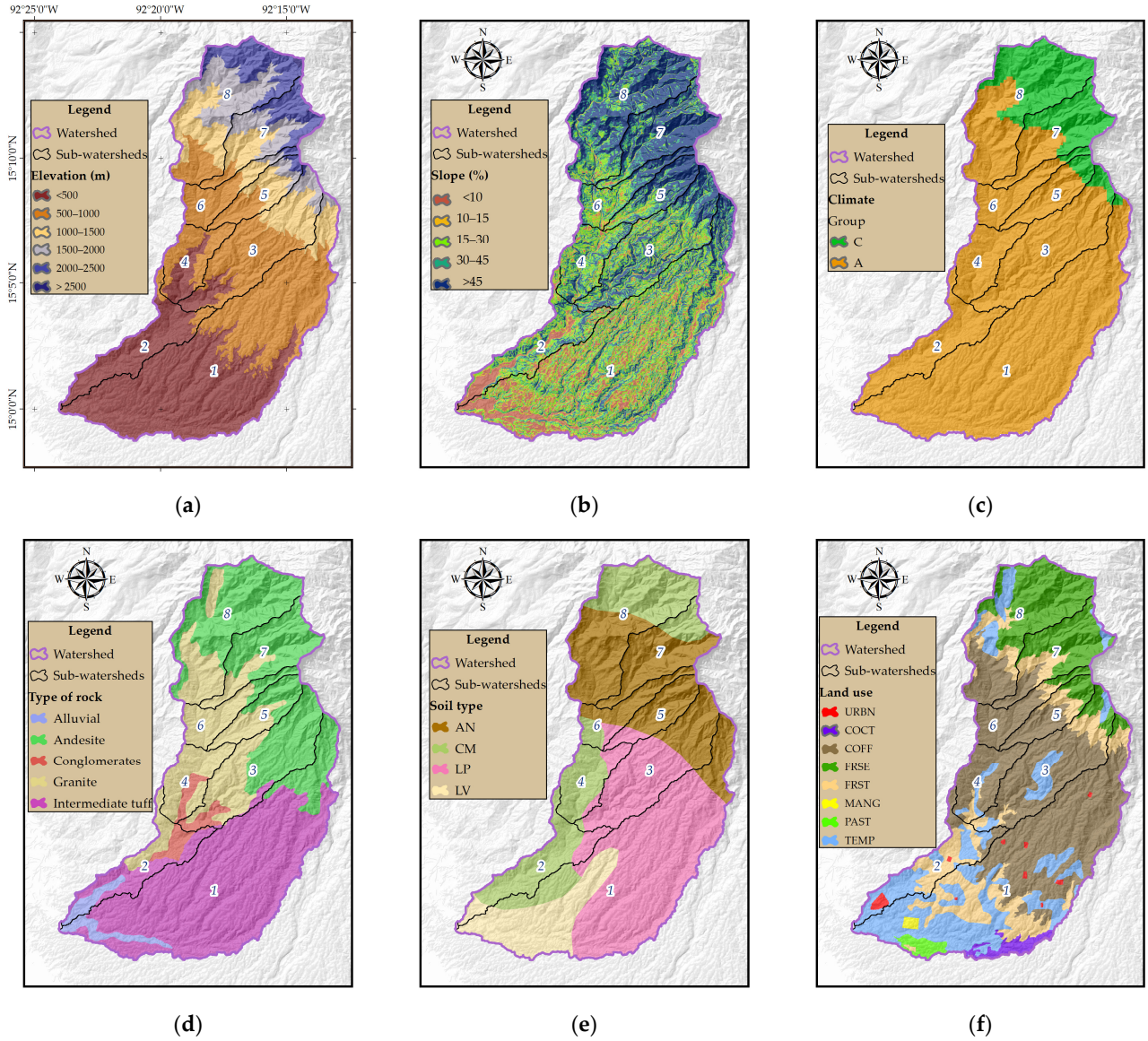

Figure 2. Main characteristics of the HRB: (**a**) elevation, (**b**) slope, (**c**) climate, (**d**) geology, (**e**) soil types, and (**f**) land uses.

2.2. Estimation of Primary and Secondary Criteria

2.2.1. Morphometry

The morphometric parameters of the HRB were calculated using a stream network at a 1:50,000 scale from the Mexican National Institute for Geography and Statistics (INEGI) [35]. The morphometric parameters were determined by applying Equations (1) and (2) proposed by Horton [37] for drainage density (D_d) and stream frequency (D_h), respectively, and Equation (3) by Strahler [38] for the mean bifurcation ratio (R_{bm}).

$$D_d = \frac{L_u}{A} \tag{1}$$

where D_d is the drainage density (number of streams km^{-2}), L_u is the total number of streams of order u in the sub-watershed, and A is the area of the sub-watershed (km^2).

$$D_h = \frac{L_{tc}}{A} \tag{2}$$

where D_h is the stream frequency (km of streams km^{-2}), L_{tc} is the total length of streams in the sub-watershed (km), and A is the area of the sub-watershed (km^2).

$$R_{bm} = \frac{\sum_{u=1}^{u_{max}} Rb_u}{u_{max}} \quad (3)$$

where R_{bm} is the mean bifurcation ratio, R_{bu} is the bifurcation ratio for each stream of order u, and u_{max} is the maximum stream order for each sub-watershed.

To assess the evolution of the watershed, the hypsometric integral (*IH*) was calculated as the cumulative area under the hypsometric curve and classified according to Strahler [39] as young ($IH > 60\%$), mature ($35\% < IH < 60\%$), and old ($IH < 35\%$). The *IH* value was calculated by applying the CalHypso tool [40]. These morphometric parameters were selected because they significantly influence watershed degradation processes, together with relief and soil characteristics [12,41].

2.2.2. Hydrology

Runoff (*Esc*) and peak flow (Q_p) values were determined using the Soil and Water Assessment Tool (SWAT) [42]. This tool was implemented by using the QSWAT3 plugin within the graphical interface of the open-source QGIS version 3.16.8 program [43]. SWAT is a semi-distributed hydrological model developed by the United States Department of Agriculture Research Service (USDA-ARS) that performs multiple simulations of the different components of the water balance in continuous time (annual, monthly, and daily) at spatial and temporal levels. The primary function is the estimation of runoff and sediment production, as well as the prediction of the impact of soil management practices on water quality in large basins with different elevations, land use/land cover, and soil types [42,44]. SWAT calculates the components of the hydrological cycle based on the water balance equation (Equation (4)) [42].

$$SW_t = SW_0 + \sum_{i=1}^{t}(R_i - Q_i - ET_i - W_i - RF_i) \quad (4)$$

where SW_t is the final soil water content (mm), SW_0 is the initial soil water content on day i (mm), t is the simulation period (days), R_i is the total precipitation (mm), Q_i is the surface runoff (mm), ET_i is evapotranspiration (mm), W_i is the amount of water that percolates into the soil profile (mm), and RF_i is the return flow (mm).

The model input data corresponds to the Digital Elevation Model (DEM) obtained from INEGI's Digital Elevation Model Version 3.0 with 15 m spatial resolution [32], a land-use map obtained through supervised classification of Landsat 5 TM satellite images (image date: 13 July 1993) with 30 m spatial resolution, a soil type map obtained from the INEGI with scale 1:1,000,000 Serie I [36], and the soil physicochemical properties through a soil profile analysis within the HRB [45].

Furthermore, the SWAT model requires meteorological variables such as precipitation, maximum and minimum temperature, solar radiation, wind speed, dew point temperature, and relative humidity. These variables can be incorporated or estimated with the WXGEN climate generator, which works based on the monthly statistics of each variable. The required data were obtained using the daily precipitation and maximum and minimum temperatures recorded at three CONAGUA meteorological stations located within the area of influence of the HRB for the period 1965–1994. These stations provided data with more than 85% completeness for these variables. Similarly, the missing data were estimated using the climatol package in R [46]. In addition, wind speed and solar radiation variables were derived from the Climate Forecast System Reanalysis (CFSR) database [47]; the maximum intensity of rain in 30 min was determined using the Chen method [48,49] and the dew point temperature was estimated based on the relationship with the minimum temperature for humid areas [50]. Monthly runoff records were obtained from CONAGUA's National Surface Water Data Bank (BANDAS) for the Huehuetan Hydrometric Station located at the

HRB outlet [51]. The SWAT model was run from 1965 to 1994 with two years of warm-up (1965–1966) to adjust the initial soil moisture content [52].

Calibration was carried out using the SWAT Calibration and Uncertainty Program (SWAT-CUP). This program provides a decision-making framework and incorporates a semi-automatic approach for sensitivity, calibration, validation, and uncertainty analyses by implementing the Sequential Uncertainty Adjustment Method (SUFI-2) algorithm [44]. The selected parameters are mainly associated with runoff production, groundwater flow, HRU definition, and soil type [53]. Therefore, the model was calibrated each month from 1967 to 1980 and was finally validated from 1981 to 1994. During these periods, the hydrometric station operated continuously, consistently recording recorded flow rates; however, it operated intermittently in subsequent years, with a recording rate of only 47.40% until 2010, when it ceased operations permanently [51].

The performance of the SWAT model was evaluated using the Coefficient of Determination (R^2), the Nash–Sutcliffe Efficiency Index (*NSE*), and the Percentage of Bias (*PBIAS*), widely used in the assessment of the results produced by hydrological models [54], following Equations (5), (6) and (7), respectively.

$$R^2 = \left[\frac{\sum_{i=1}^{n} (O_i - O_m)(S_i - S_m)}{\sum_{i=1}^{n} (O_i - O_m)^2 \sum_{i=1}^{n} (S_i - S_m)^2} \right]^2 \quad (5)$$

$$NSE = 1 - \frac{\sum_{i=1}^{n} (O_i - S_i)^2}{\sum_{i=1}^{n} (O_i - O_m)^2} \quad (6)$$

$$PBIAS = \frac{\sum_{i=1}^{n} O_i - S_i}{\sum_{i=1}^{n} O_i} \times 100 \quad (7)$$

where O_i is the observed flow, S_i is the simulated flow on month i, O_m is the average of the observed flow, and S_m is the average of the simulated flow. R^2 ranges from 0 to 1, where 0 indicates no correlation and 1 corresponds to a perfect correlation and a lower error variance. *NSE* ranges from $-\infty$ to 1, where values ≤ 0 indicate that the model is unreliable, and values closer to 1 denote a perfect fit between observed and simulated data. The best value of *PBIAS* is 0, while positive and negative values correspond to model underestimation and overestimation, respectively.

2.2.3. Hillslope Stability and Soil Water Saturation Indices

Hillslope stability and soil water saturation indices were obtained with the Stability Index Mapping (SINMAP) version 2.0 model for ArcGIS 9.3 [55] using a digital elevation model with 15 m resolution [32], supplemented with field information on variables related to the geotechnical characteristics of soil, precipitation, and inventory of landslides.

The SINMAP model combines a uniform-regime hydrological model sensitive to relief variations with an infinite slope stability model [55]. Based on the DEM, the mechanical and hydrogeological properties of the study area, and the inventory of landslides [56], SINMAP performs terrain stability classification based on the spatial variation in slopes and their contributing area [57]. Hillslope stability values vary between 0 (most unstable) and 1 (least unstable). The accuracy of the instability index map produced by SINMAP was evaluated using the Receiver Operating Characteristic (*ROC*) curve [58], which is effective for representing the quality of detection, probabilistics, and forecasting systems [59]. The inventory of landslides was compiled from 2005 to 2021 based on field research and a visual inspection of Landsat 7 and Sentinel satellite images (https://earthexplorer.usgs.gov/, accessed on 15 February 2022). Subsequently, 281 landslides were identified, primarily located in the highlands of the HRB.

The area under the ROC curve (*AUC*) represents the accuracy evaluation index of the model; it ranges from 0.5 (random prediction, represented by a diagonal straight line) to 1.0 (perfect prediction) and can be used for model comparison [60].

The values obtained for each sub-watershed were classified as Unstable (*I*), Slightly stable (*LE*), or Stable (*E*) based on the hillslope stability index, or as Dry (*Se*), Wet (*H*), or Saturated (*Sa*) based on the soil water saturation index.

2.2.4. Change in Land Use

The Normalized Difference Vegetation Index (*NDVI*) was used to estimate land-use changes based on raster images from Landsat 5 TM (image date: 13 July 1993) and Landsat 8 OLI (image date: 20 July 2013). *NDVI* values are useful in the classification of land uses [61]; for this reason, Equation (8) proposed by Hayes [62] was used.

$$NDVI = \frac{\rho_{NIR} - \rho_R}{\rho_{NIR} + \rho_R} \quad (8)$$

where *NDVI* is the Normalized Difference Vegetation Index, and ρ_{NIR} and ρ_R correspond to the surface reflectance of the near-infrared and red bands.

Additionally, images were reclassified as low (*VB*), medium (*VM*), and high (*VA*) vegetation. Subsequently, land-use changes were calculated for sub-watersheds and used as sub-criteria.

2.2.5. Socioeconomic Conditions

The sub-criteria for socioeconomic conditions were obtained from the National Council for the Evaluation of Social Development Policy (CONEVAL, after the name in Spanish), specifically population density (*DP*) and the margination index (*IM*) [63]. The margination index is defined as the percentage of the population that lacks essential services [64]. The social vulnerability index (*IVS*) considers factors such as health status, education level, housing, and gender [65]. Values were obtained at the municipal level, and the occupied area in the sub-watersheds was estimated.

The HRB includes the municipalities of Motozintla, Huehuetan, and Tapachula. Tapachula comprises the largest area, with 233.65 km^2, representing 73.18% of the watershed. According to INEGI's 2010 National Census, Huehuetan includes 183 communities with a total population of 30,677 inhabitants, and Huehuetán, the most populated town, is home to 7755 people [64].

Adequate infrastructure, including roads, electricity, drinking water, and healthcare services, is located in the lower part of the basin. However, these services are largely insufficient in the upper and middle sections, and many communities lack essential infrastructure, particularly road access.

2.3. Multicriteria Evaluation with the ANP Model

Multicriteria decision-making (MCDM) consists of the following sequence of steps to solve a problem: identify the problem, develop alternatives to manage/solve the problem, evaluate these alternatives, and select the best alternative. Decision-making is intuitive when issues involve a single criterion and only the alternative with the greatest preference is selected. However, when different criteria and sub-criteria are evaluated, it becomes a complex problem that requires the application of more sophisticated methods [66].

The Analytic Network Process (ANP), a general form of the Analytic Hierarchy Process (AHP), considers the dependence between a hierarchy of elements [66]. In addition, the ANP model considers the interrelation and dependence between the elements involved [67].

The first step of the ANP model allows the identification of the elements in the hierarchy related to the target function. The second step seeks to integrate the interfactorial dominance supermatrix (Equation (9)), identifying the relationships and feedback between the elements to determine any potential influence. Using pairwise comparison matrices, the third step determines the magnitude of the impact of elements by estimating the importance of one element compared to another based on the alternatives. This implies converting

qualitative data into quantitative data through Saaty's comparison scale based on expert opinions and judgments that will provide input information for the model [68].

$$W = \begin{array}{c} \begin{array}{cccc} C_1 & & C_2 & \cdots & C_m \\ e_{11} \cdots e_{1n_1} & & e_{21} \cdots e_{2n_2} & \cdots & e_{m1} \cdots e_{mn_m} \end{array} \\ \begin{array}{c} \\ C_1 \\ \\ \\ \\ C_2 \\ \\ \\ \\ \vdots \\ \\ C_m \\ \\ \\ \end{array} \begin{array}{c} \begin{array}{c} e_{11} \\ e_{12} \\ \vdots \\ e_{1n_1} \end{array} \\ \begin{array}{c} e_{21} \\ e_{22} \\ \vdots \\ e_{2n_2} \end{array} \\ \begin{array}{c} \\ \vdots \\ \\ \end{array} \\ \begin{array}{c} e_{m1} \\ e_{m2} \\ \vdots \\ e_{mn_m} \end{array} \end{array} \begin{bmatrix} W_{11} & W_{12} & \cdots & W_{1m} \\ W_{21} & W_{22} & \cdots & W_{2m} \\ \vdots & \vdots & \vdots & \vdots \\ W_{m1} & W_{m2} & & W_{mm} \end{bmatrix} \end{array} \quad (9)$$

where C_m denotes the m-th criterion, e_{mm} denotes the n-th element in the m-th criterion, and W_{ij} is the principal eigenvector of influence of the elements compared in the j-th and i-th criteria. Thus, if the j-th criterion does not influence the i-th criterion, then $W_{ij} = 0$. Therefore, the shape of the supermatrix depends on the network structure between the elements and their interactions. The blocks W_{ij} represent the supermatrix and are represented by Equation (10) [18].

$$W_{ij} = \begin{bmatrix} w_{i_1 j_1} & w_{i_1 j_2} & \cdots & w_{i_1 j_{n_j}} \\ w_{i_2 j_1} & w_{i_2 j_2} & \cdots & w_{i_2 j_{n_j}} \\ \vdots & \vdots & \vdots & \vdots \\ w_{i_{n_i} j_1} & w_{i_{n_i} j_2} & \cdots & w_{i_{n_i} j_{n_j}} \end{bmatrix} \quad (10)$$

The ANP model allows the decision maker to evaluate consistency analytically through the consistency index (CI) (Equation (11)).

$$CI = \frac{\lambda_{max} - n}{n - 1} \quad (11)$$

where λ_{max} is the principal eigenvalue (λ) from the supermatrix and n is the number of elements in the analysis.

The correctness of the consistency analysis and the judgment scale are determined using the consistency ratio (CR), which measures the consistency of the paired-comparison matrices (Equation (12)).

$$CR = \frac{CI}{RCI} \quad (12)$$

where RCI is the random consistency index, the value of which can be obtained from [68] based on the matrix order.

In the analysis of the paired-comparison matrices, the result is consistent when $CR < 0.10$ [68]. Therefore, any result exceeding this limit indicates an inconsistency in value judgments, and the analysis must be reevaluated. Finally, the limiting supermatrix is derived from the weighted supermatrix, where the values in each column represent the weights of the criteria, sub-criteria, and alternatives [67].

2.3.1. Identification of Network Elements

Based on the information from the watershed and field studies, watershed degradation was associated with the most important criteria related to watershed degradation (Figure 3). Furthermore, the opinions of four watershed management experts were considered to rank the variables of greatest importance for each criterion (6 criteria and 18 sub-criteria).

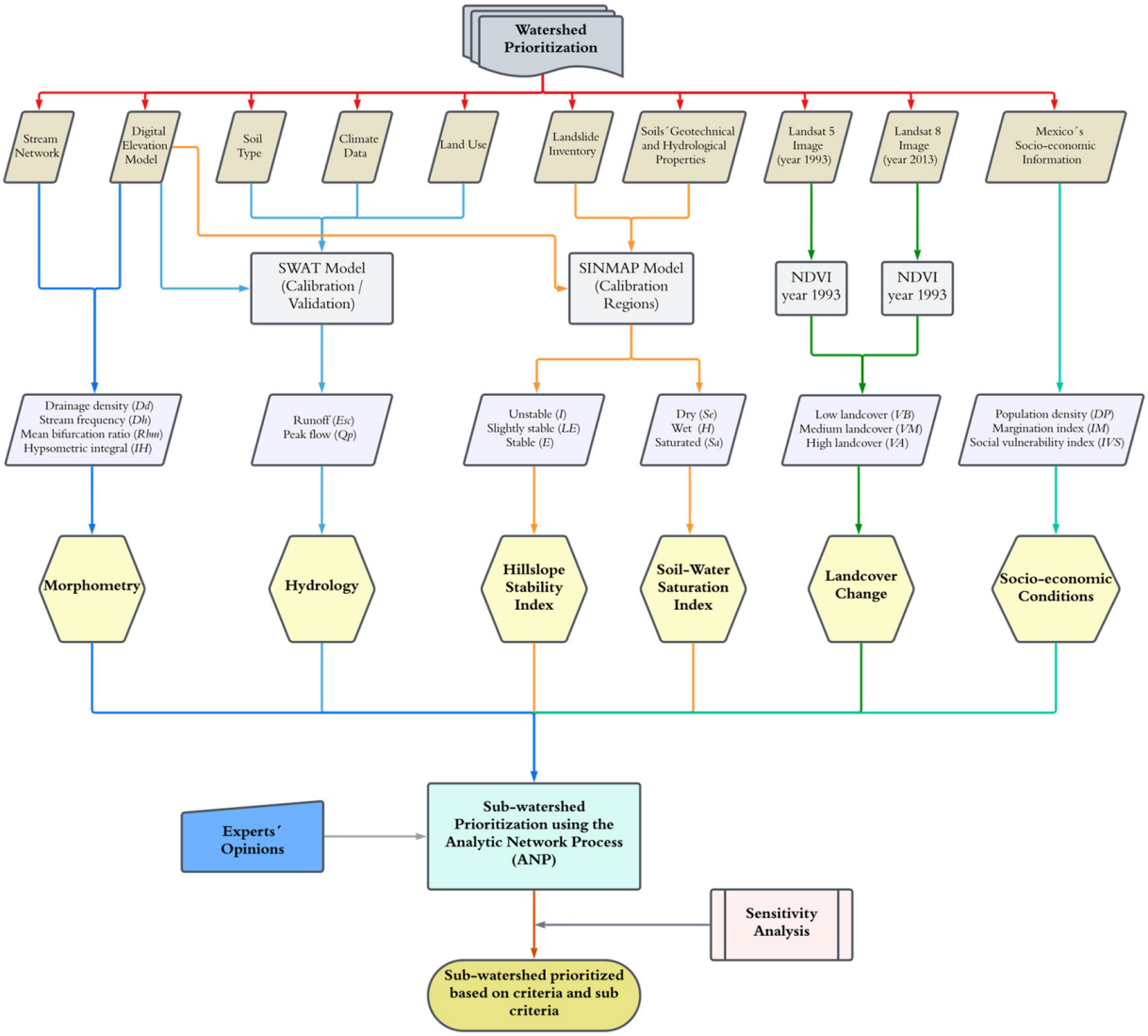

Figure 3. General research flowchart for HRB sub-watershed prioritization.

2.3.2. Network Structure

The network of the ANP model was structured considering the interdependence or feedback between the criteria, sub-criteria, and possible alternatives (Figure 4).

2.3.3. Construction of Original, Weighted, and Limit Supermatrices

The influence of each element was assessed using the Saaty fundamental comparison scale [69]. Pairwise comparison matrices were constructed based on the results of each sub-criterion and the overarching supermatrix of influences. Subsequently, a weighted supermatrix was developed, followed by calculating the limit supermatrix.

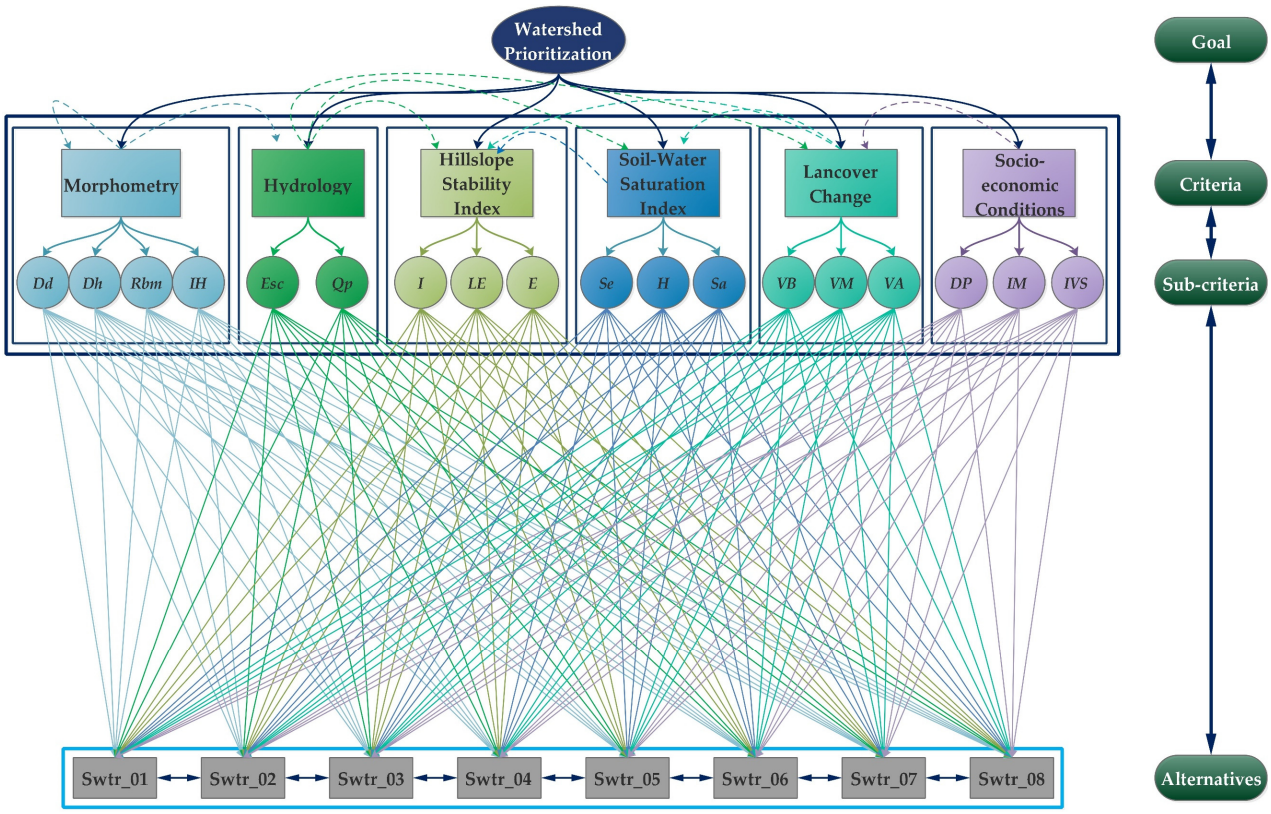

Figure 4. General scheme of the network structure of the ANP model.

2.3.4. Sensitivity Analysis of the ANP Model

The last step in the decision-making process is the "sensitivity analysis", which involves a slight modification of the numerical values of the sub-criteria to assess how they impact the outcome of the priorities [70]. However, due to the complex structure of the ANP model network, this step is rarely carried out [15]. This analysis is performed because the priorities depend on the assigned weights given to the sub-criteria based on the expert opinion from pairwise comparisons. Therefore, these inaccuracies can change the priorities of the sub-watershed [71,72]. The sensitivity analysis shows how much these priorities vary when the initial values are modified. In this way, we can reach a reasonable conclusion about the reliability of the results [73].

The sensitivity analysis was carried out using the Super Decisions® software version 3.2.0, considering the four sub-criteria that have the greatest influence on the decision process: 1. Runoff (*Esc*), 2. Low vegetation (VB), 3. Unstable (I), and 4. Peak flow (Q_p).

3. Results

3.1. Analysis of the Criteria and Sub-Criteria Used

3.1.1. Morphometry Criterion

Morphometric parameters are directly related to watershed degradation and the growth of the stream network [12,41]. Table 1 shows the main morphometric parameters of the sub-watersheds, including area (A), perimeter (P), length of the main channel (L_{mc}), total length of the streams (L_{st}), slope of the main channel (P_{mc}), mean sub-watershed slope (P_{sm}), altitudinal range (AL), altitudinal difference (AD), total number of streams (N_s), time of concentration (T_c), and order number of the main channel (O).

Table 1. Principal morphometric parameters of the sub-watersheds.

Sub-Watershed	A (km^2)	P (km)	L_{mc} (km)	L_{st} (km)	P_{mc} (%)	P_{sm} (%)	Altitude (m a.s.l.)			AD (m)	N_s	T_c (h)	O
							High	Minimum	Mean				
Swtr 01	129.50	97.72	40.96	618.74	4.71	25.75	30	1960	469	1930	1495	3.75	VI
Swtr 02	25.52	53.18	16.79	99.93	3.75	23.33	30	660	246	630	196	2.06	IV
Swtr 03	41.59	48.02	19.41	215.15	11.42	41.42	213	2430	903	2217	505	1.50	V
Swtr 04	16.57	26.78	9.57	83.94	6.69	32.87	210	850	529	640	192	1.07	VI
Swtr 05	14.23	26.52	10.02	76.02	20.06	57.67	510	2520	1205	2010	179	0.73	IV
Swtr 06	14.25	32.20	10.94	83.28	19.38	43.07	510	2630	960	2120	207	0.79	VI
Swtr 07	25.92	37.48	13.23	145.28	15.12	66.95	660	2660	1745	2000	415	1.00	V
Swtr 08	51.70	47.20	18.03	279.75	11.26	58.12	660	2690	1651	2030	738	1.42	VI

This information was used to calculate drainage density (D_d), stream frequency (D_h), and mean bifurcation ratio (R_{bm}). These parameters have the greatest impact on the watershed degradation processes; therefore, they allow prioritizing areas with greater certainty without increasing the number of sub-criteria [69,74].

Figure 5 shows the hypsometric curve (*HC*) of each sub-watershed according to relative elevation (*h*/*H*) and relative area (*a*/*A*). The area below the *HC* is the hypsometric integral (*IH*). Total elevation (*H*) is the highest altitude, total area (*A*) is the total surface area of the watershed, and area (a) is the surface area within the watershed above a given altitude (*h*) [39]. This facilitates determining the evolution and effect of the area–altitude relationship on erosion over time. *IH* was calculated using the integrated area under the hypsometric curve.

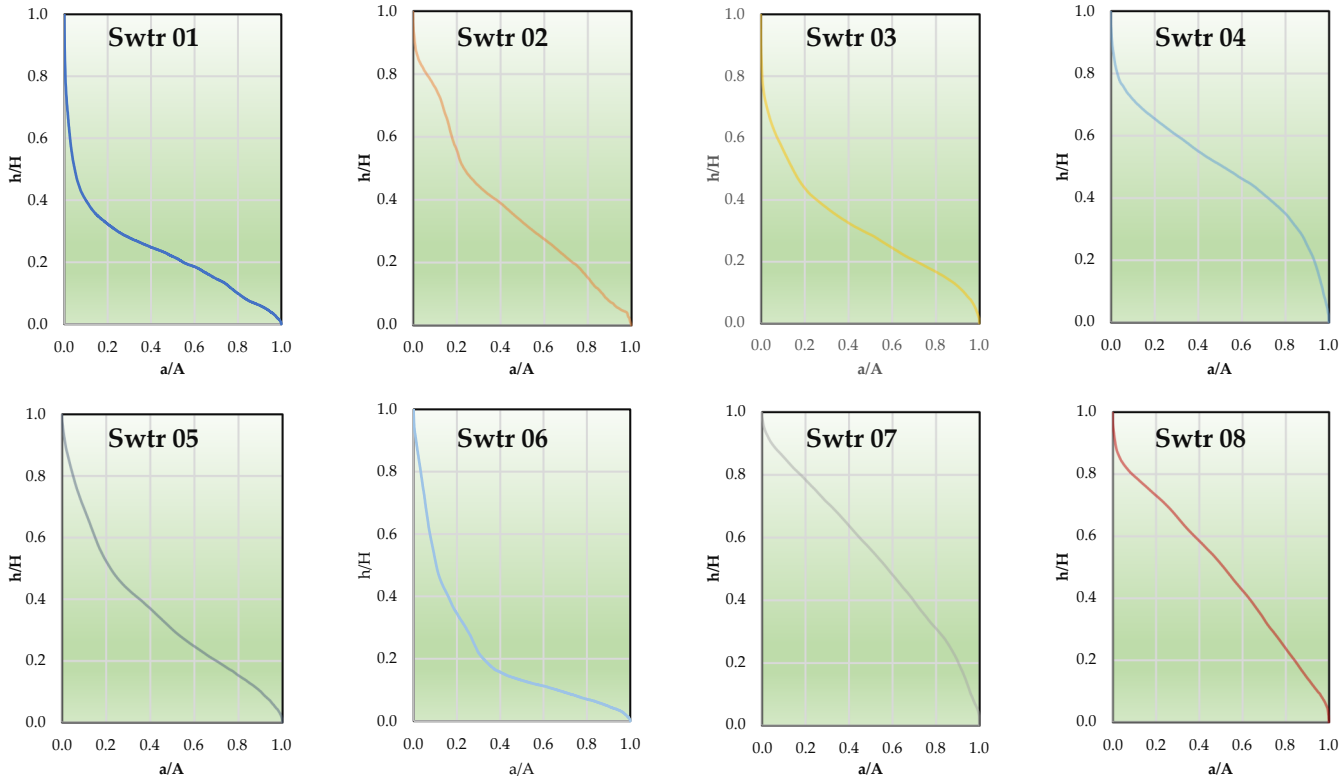

Figure 5. Hypsometric curve for the sub-watersheds of the HRB.

Figure 6 shows the drainage density (D_d), stream frequency (D_h), mean bifurcation ratio (R_{bm}) sub-criteria, and the hypsometric integral (*IH*) for the HRB morphometry criterion used in the ANP model (see Table S1).

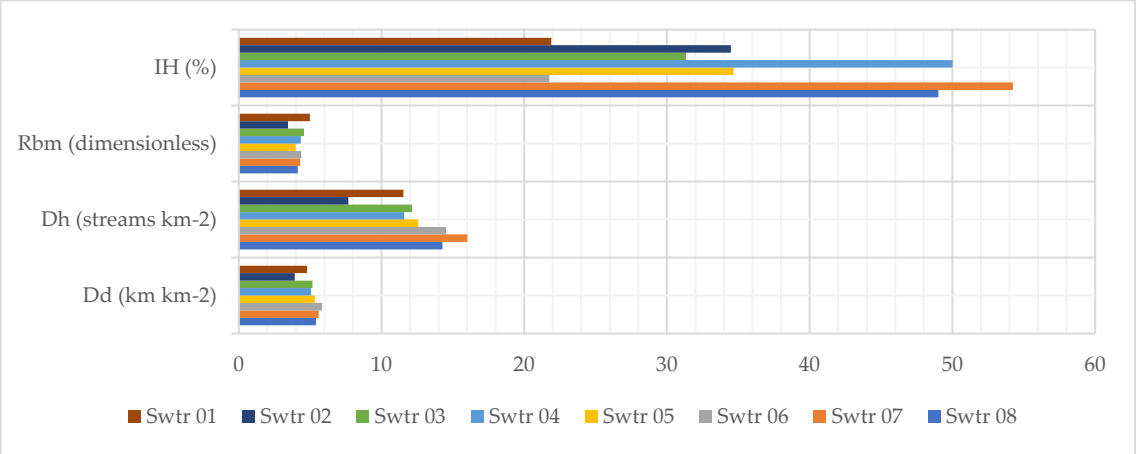

Figure 6. Morphometry sub-criteria for the HRB sub-watersheds.

3.1.2. Hydrology Criterion

The magnitude of runoff (*Esc*) and peak flow (Q_p) influence sediment transport capacity and their impact on hillslope erosion. Similar processes are related to soil degradation and the increase in the stream network [1]. The SWAT model was applied in the HRB from 1965 to 1994 to obtain *Esc* and Q_p values. During calibration, the most sensitive parameters were the depth of the impermeable layer (DEP_IMP), lateral flow travel time (LAT_TTIME), curve number (CN2), time to aquifer recharge (GW_DELAY), baseflow alpha factor for bank storage (ALPHA_BNK), deep aquifer percolation (RCHRG_DP), soil depth (SOL_Z), and soil evaporation compensation (ESCO).

Figure 7 shows the monthly streamflow behavior of the hydrometric station located at the HRB outlet and the streamflow simulated by the SWAT model. The observed and simulated monthly mean streamflow values were 27.88 $m^3\ s^{-1}$ and 28.92 $m^3\ s^{-1}$, respectively.

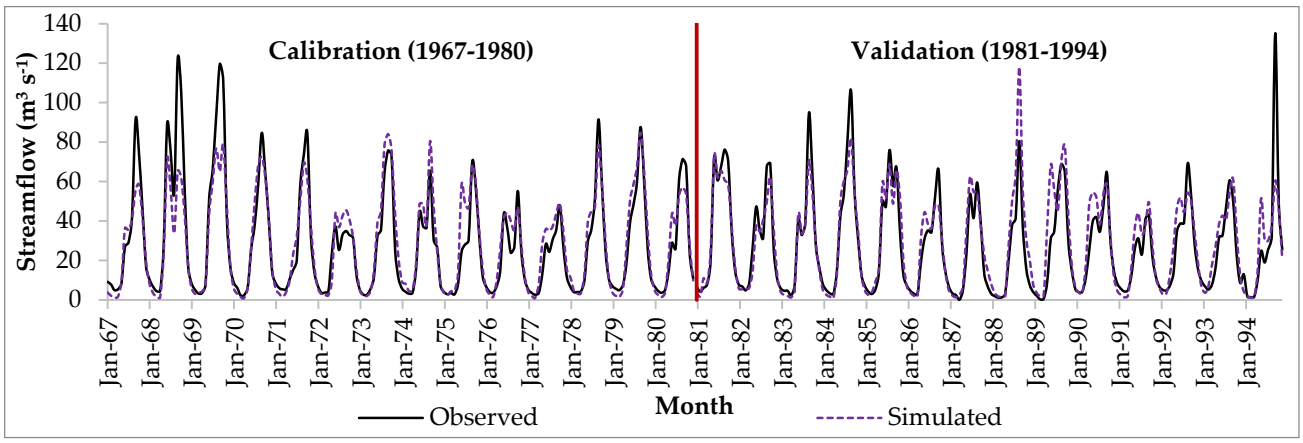

Figure 7. Comparison of the simulated and observed streamflow in the HRB.

The comparison between the observed and simulated streamflow by the SWAT model using the performance evaluation metrics (R^2, *NSE*, and *PBIAS*) indicates a good correlation according to the criteria of Moriasi et al. [54] (Table 2). Therefore, the model can be successfully implemented to simulate the monthly streamflow in the HRB.

Table 2. Calibration and validation results for the SWAT model.

Period	R^2	Classification	*NSE*	Classification	*PBIAS*	Classification
Calibration	0.84	Good	0.83	Good	−0.30	Very good
Validation	0.81	Good	0.80	Good	−7.37	Good

Subsequently, the runoff (*Esc*) and peak flow (Q_p) values calibrated and validated with the SWAT model were used for the hydrology criterion (see Table S1). Figure 8a,b shows *Esc* and Q_p values for each sub-watershed.

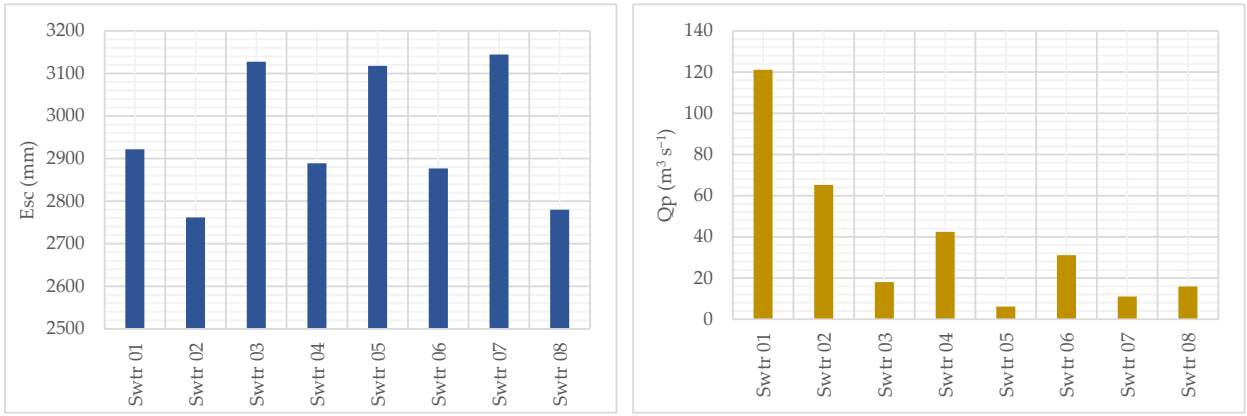

(**a**) (**b**)

Figure 8. Hydrology sub-criteria for the sub-watersheds: (**a**) runoff and (**b**) peak flow.

3.1.3. Hillslope Stability and Soil Water Saturation Criteria

The proximity to the Tacaná volcano influences the relief of the HRB. Therefore, the soil conditions are shaped by processes that have occurred over millions of years, affecting the steep relief, which produces susceptibility to landslides in the watershed highlands [26]. The stability analysis indicates that 64.28% of the watershed surface is stable. However, hillslope stability is proportional to its relief, where stable areas with a gentle slope are in the lowlands, while the highlands are unstable due to steep slopes and abrupt relief. In unstable regions, the risk of landslides increases with the occurrence of short-duration intense rainfall events [75,76].

The stability index (*SI*) classified the HRB into six classes (Figure 9a). According to the spatial distribution of the soil water saturation index, saturated areas are located in the lowlands, close to streams. However, the association of slope, rainfall, land use, and soil in the highlands increases landslide susceptibility (Figure 9b).

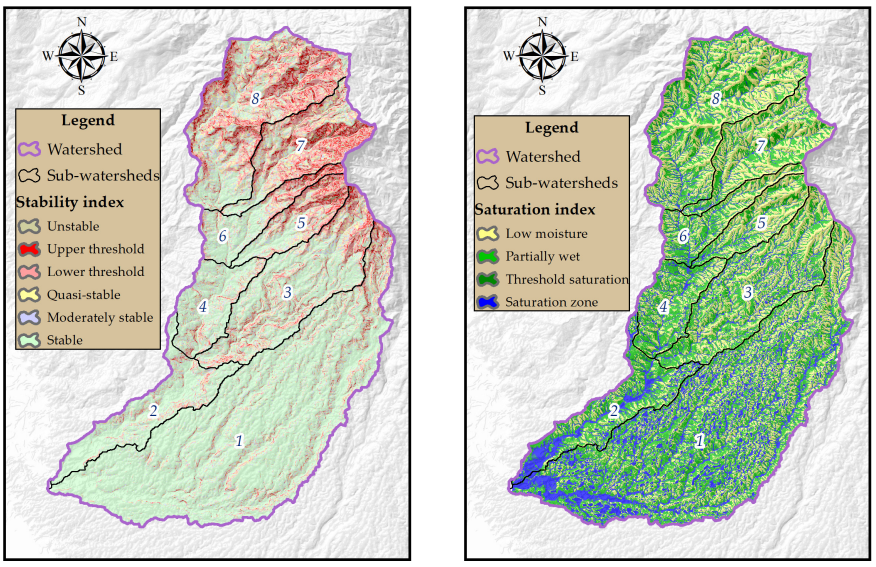

(**a**) (**b**)

Figure 9. Spatial distribution of (**a**) the stability index and (**b**) the soil water saturation index in the HRB.

The SINMAP hillslope stability map was validated using a landslide inventory, showing an accuracy of 85.60% on the ROC curve (Figure 10). This indicates that SINMAP is an excellent tool for predicting areas susceptible to landslides (for additional details, refer to Table S1).

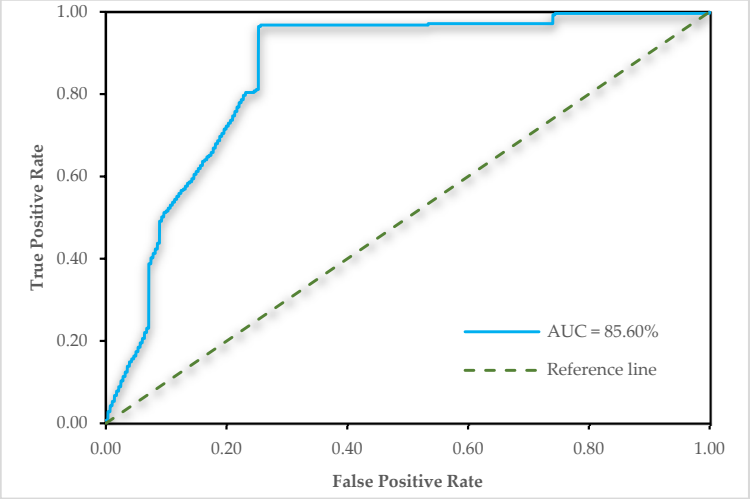

Figure 10. ROC curve for the hillslope stability map of the HRB.

Additionally, the area (in hectares) of each sub-watershed was classified as Unstable (*I*), Slightly Stable (*LE*), or Stable (*E*), according to the stability index (Figure 11a), and as Dry (*Se*), Wet (*H*), or Saturated (*Sa*), according to the soil water saturation index (Figure 11b).

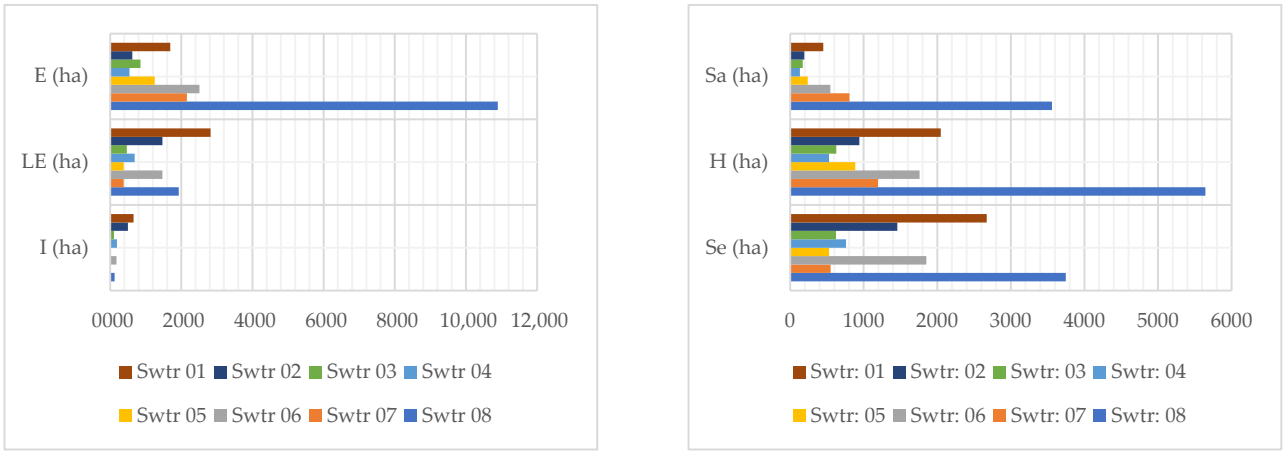

(**a**) (**b**)

Figure 11. Area of the sub-watershed classes in the HRB according to (**a**) the stability index and (**b**) the soil water saturation index.

3.1.4. Land-Use Change Criterion

The *NDVI* variations between 1993 and 2013 indicate a reduction in high vegetation (VA), with values near 10% (Figure 12a–c). In the highlands, this change is primarily driven by the conversion of areas of temperate and tropical forests to agriculture on hillslopes [77]. In addition, 7.8% increases in medium vegetation (*VM*) related to shaded coffee plantations have contributed to the decline in high vegetation in recent years.

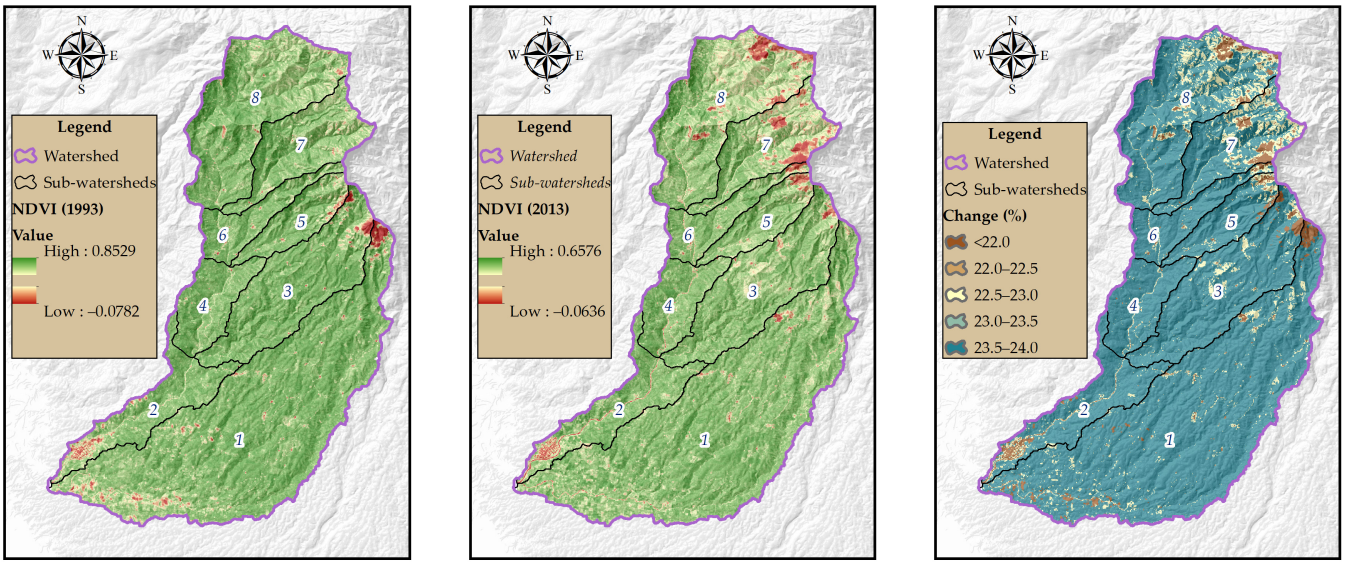

Figure 12. Spatial variation in *NDVI* values: (**a**) 1993, (**b**) 2013, and (**c**) percentage of land-use change in the HRB over the study period.

Subsequently, the change in the *NDVI* was used to calculate the change for low (*VB*), medium (*VM*), and high (*VA*) vegetation. Positive values indicate a gain in land cover, while negative values indicate a loss within the class (see Table S1). The temporal variation shows that high vegetation (*VA*) has declined in all the sub-watersheds, while medium or low vegetation has increased. Figure 13 shows changes in the area covered by each vegetation type (in hectares) in each sub-watershed.

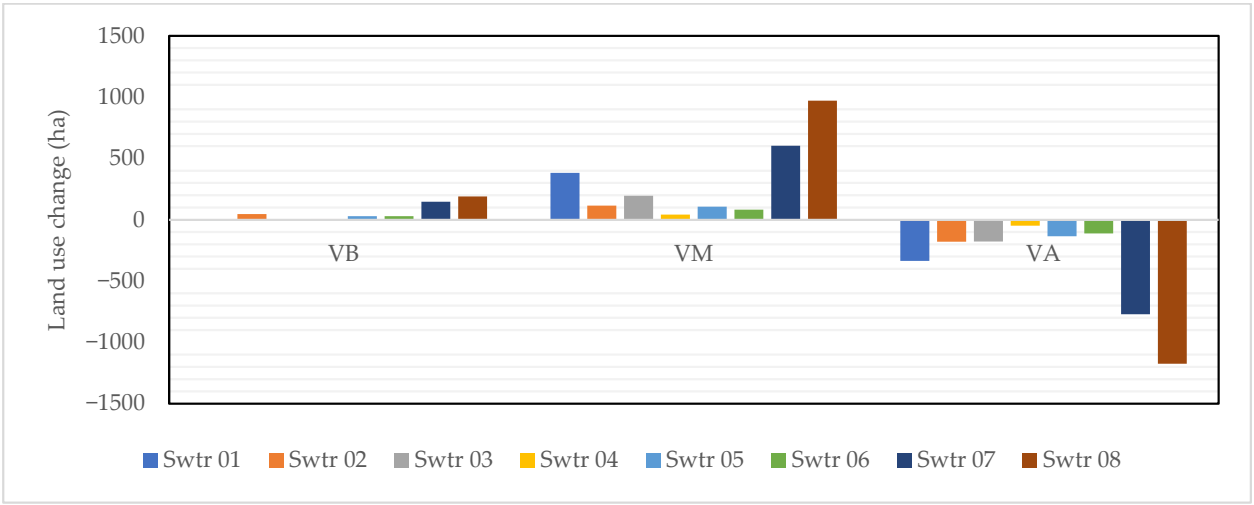

Figure 13. Land-use change sub-criterion for the sub-watersheds in the HRB.

3.1.5. Values for the Socioeconomic Criterion

Economic data for the HRB [63] indicate that population density (*DP*) ranges from 0.25 to 3.6 inhabitants km^{-2} (Figure 14a); the mean margination index (*IM*), from 14.9 to 18.55 (Figure 14b); and the social vulnerability index (*IVS*), from 0.43 to 0.55 (Figure 14c) [30] (see Table S1).

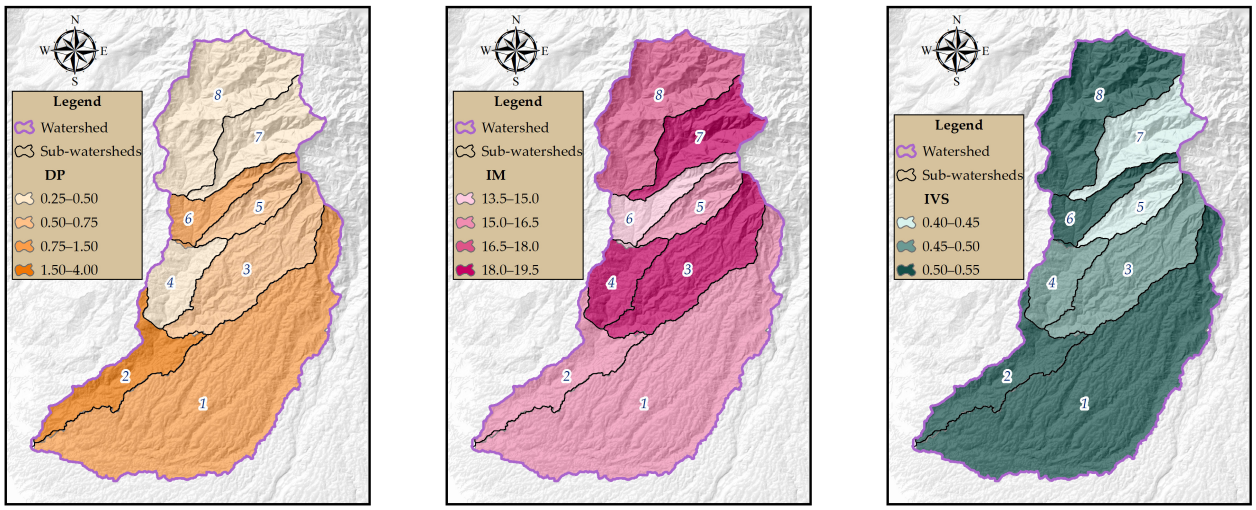

(**a**) (**b**) (**c**)

Figure 14. Spatial variation in (**a**) *DP*, (**b**) *IM*, and (**c**) *IVS* in the HRB.

Although socioeconomic conditions are adequate for communities in the lowlands of the watershed, a significant social gap in the highlands restricts the development of rural communities. The low education level generates a lack of knowledge and neglect of the environment, which influences the alterations of biophysical conditions and affects the conservation of soils and forests in the HBR. The latter is evident in cases where low-production crops are cultivated in areas with forestry potential.

3.2. Ranking the Criteria and Sub-Criteria

The application of the ANP model facilitated the identification of the most important criteria and sub-criteria involved in the degradation of the watershed (Tables S2–S4). These criteria are ranked by importance, along with their respective weights: (1) hydrology (20.62%), (2) land-use change (19.82%), (3) soil water saturation index (15.59%), (4) morphometry (15.17%), (5) hillslope stability index (14.61%), and (6) socioeconomic conditions (14.20%). Regarding the degradation processes, six sub-criteria were the most important, ranked according to their priority: (1) runoff (*Esc*), (2) low vegetation (*VB*), (3) unstable (*I*), (4) peak flow (Q_p), (5) saturated (*Sa*), and (6) population density (*DP*). This information is illustrated in Figure 15.

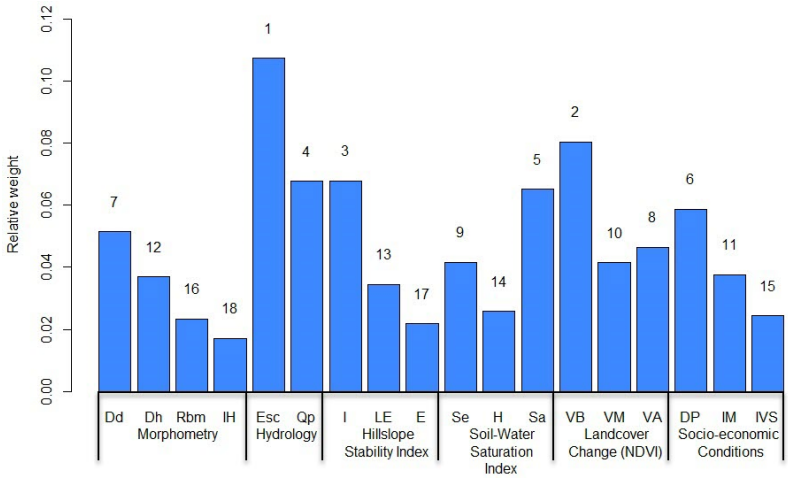

Figure 15. Ranking of ANP sub-criteria for the prioritization of sub-watersheds in the HRB.

3.3. Sub-Watershed Prioritization

Sub-watershed prioritization using the ANP model is shown in Figure 16. Sub-watersheds with priority one and two correspond to Swtr 08 and Swtr 07, located in the highlands, covering an area of 51.70 km^2 (16.19%) and 25.92 km^2 (8.12%), respectively. Sub-watersheds Swtr 01 and Swtr 02, with priority ranks three and four, are located in the watershed lowlands, covering an area of 129.50 km^2 (40.56%) and 25.52 km^2 (7.99%). Finally, the sub-watersheds located in the middle part have low priority, ranked as follows (in descending order): Swtr 03 (13.03%), Swtr 04 (5.19%), Swtr 05 (4.46%), and Swtr 06 (4.46%); together these sub-watersheds comprise a total area of 86.63 km^2 (27.13%).

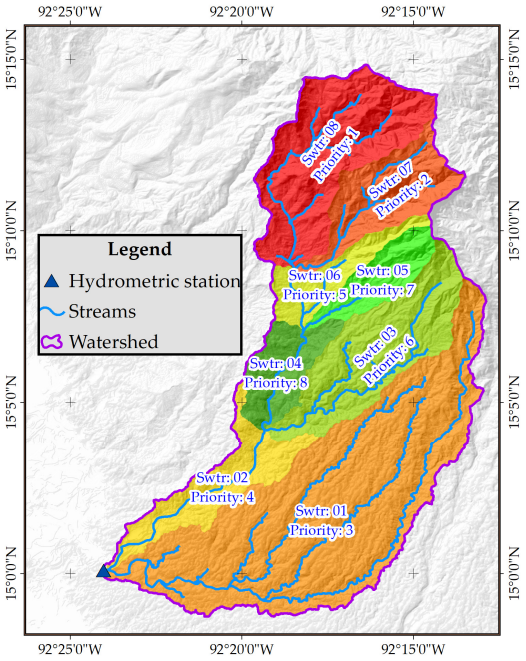

Figure 16. Sub-watershed prioritization in the HRB.

We found a strong correlation between the hillslope stability index and land-use change. The two sub-watersheds with the highest priority levels exhibit high values for these sub-criteria. In contrast, sub-watersheds with lower priorities are linked to increased runoff and land-use alterations, mainly because they are located in densely populated areas and have a mixture of low and medium vegetation. This region hosts the largest agricultural area, which cultivates corn, soybean, oil palm, mango, and other tropical crops [28].

3.4. Sensitivity Analysis

The sensitivity analysis indicated the convenience of slightly modifying the values of the sub-criteria to observe the impact of this change on the priorities [70]. However, this is rarely carried out due to the complex structure of the network of the ANP model [15]. This analysis was conducted because the priorities depended on the weight assigned to the sub-criteria based on expert opinions through pairwise comparisons; therefore, these inaccuracies can influence the priority assigned to sub-watersheds [71]. The sensitivity analysis showed the extent to which these priorities can vary when the initial values are modified. This allows us to judge whether the results are robust and stable or not [73].

The sensitivity analysis used a default value, $\alpha = 0.5$, but it was possible to use values ranging from 0 to 1 [78]. The α parameter provides a measure for comparative judgments from the variations in priority vectors about each specific sub-criterion. Therefore, the variation in the α parameter showed the sensitivity with which a given sub-criterion modified the priorities of sub-watersheds. According to Dobrea et al. [78], we selected a

50% linear decrease/increase in the original value of the selected sub-criteria, equivalent to $0.25 < \alpha < 0.75$ [78].

Table 3 shows the variation in the weight for each sub-criterion in the sensitivity analysis when its initial α value was decreasing/increasing by 50%. Reducing the weight of the four most important sub-criteria did not produce significant variations in sub-watershed prioritization. For instance, a 4.53% reduction in runoff was found, while low vegetation showed the most significant increase, 6.54%. The maximum flow value did not change considerably; it only varied −0.54% when its initial value decreased by 50%.

Table 3. Sensitivity analysis with the most important sub-criteria. Values in (%).

Alternatives	Runoff (*Esc*)		Low Vegetation (*VB*)		Unstable (*I*)		Peak Flow (Q_p)	
	α = 0.25	α = 0.75	α = 0.25	α = 0.75	α = 0.25	α = 0.75	α = 0.25	α = 0.75
Swtr_01	0.00	−7.64	6.25	−43.06	1.39	−16.67	0.00	2.08
Swtr_02	0.82	−6.56	0.00	−3.28	2.46	−33.61	−2.46	22.13
Swtr_03	−4.04	19.19	5.05	−37.37	−1.01	5.05	−2.02	17.17
Swtr_04	−1.19	20.24	3.57	−20.24	3.57	−30.95	0.00	5.95
Swtr_05	−3.00	20.00	1.00	−11.00	−1.00	0.00	1.00	−8.00
Swtr_06	−0.99	11.88	1.98	−8.91	1.98	−14.85	0.00	9.90
Swtr_07	1.27	−7.59	−5.06	37.34	−1.90	25.32	1.90	−16.46
Swtr_08	2.60	−19.27	−6.25	42.19	−3.13	31.77	1.04	−14.58
Total	−4.53	30.25%	6.54	−44.33	2.37	−33.94	−0.54	18.20

A 50% increase in the weighting results (α = 0.75) produced greater variability in priorities (Table 3), as shown by the maximum global ranges of −44.33% and 30.25% for runoff and low vegetation, respectively. Additionally, instability showed a 33.94% decrease and a peak flow of 18.20%.

The changes were insignificant for α values of 0.50 to 0.25, and the priorities remained unchanged (Figure 17). However, with a 50% increase in the original value (α = 0.50 to 0.75), this variation only slightly affected the priorities. For instance, in the classification of the four top-priority sub-watersheds, the ranks of runoff and instability were modified; additionally, the priority rank of sub-watershed 02 changed from four to five.

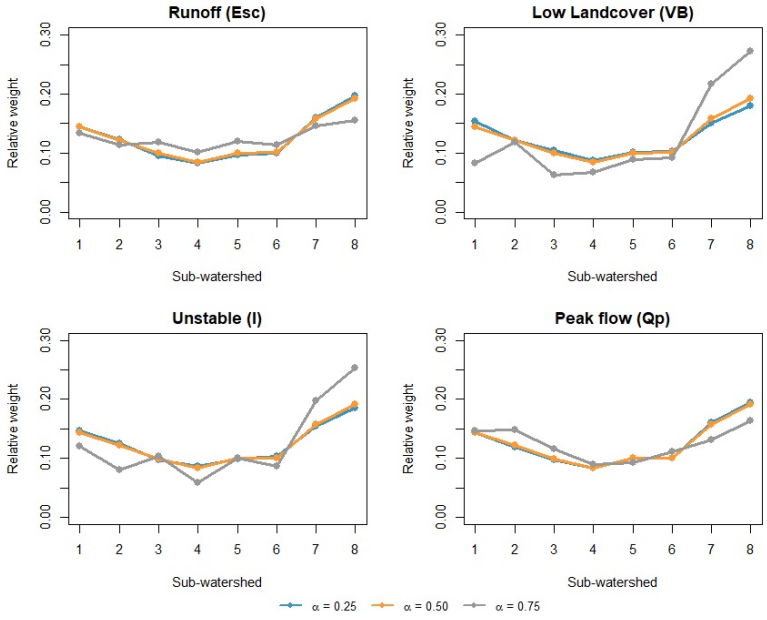

Figure 17. Sensitivity analysis considering the four sub-criteria with the highest priority.

Based on the sensitivity analysis, the changes in sub-watersheds from the highlands are reflected in the lowlands. For example, there is an inverse relation for runoff between Swtr 08 (−19.27%) and Swtr 03 (19.19%) and a direct relation between Swtr 07 (−7.59%) and Swtr 01 (−7.64%). This implies that the changes associated with expert opinions concerning the degradation of the watershed will increase or decrease according to the dependency and feedback between the sub-criteria.

4. Discussion

The HRB was divided into eight sub-watersheds using the SWAT model, following Pfafstetter's methodology [31]. Subsequently, these sub-watersheds were evaluated based on criteria and sub-criteria related to morphometry, hydrology, stability index, soil water saturation index, land-use change, and socioeconomic conditions.

In the case of the morphometry criterion, the sub-watersheds exhibit a high drainage density (D_h), mainly in the highlands (Swtr 06, Swtr 07, and Swtr 08). This suggests a close relationship between steep slopes and susceptibility to landslides. Stream frequency (D_d) affects soil fragility related to water erosion; thus, soil degradation is proportional to stream frequency [79], particularly in areas with impermeable materials, low infiltration capacity, sparse vegetation, and rugged relief [38]. The mean bifurcation ratio (R_{bm}) influences torrentiality; as the bifurcation increases, the runoff concentration time decreases, affecting the responses of the drainage system to floods [69]. Hypsometric integral (*IH*) values indicate that the sub-watersheds are between the maturity and senescence phases, with mature sub-watersheds being the most exposed to degradation [38].

For the hydrology criterion, the highest runoff (*Esc*) values were recorded for Swtr 07, primarily due to its morphometric characteristics and rainfall conditions, followed by Swtr 03 and Swtr 05. In the case of peak flow (Q_p), sub-watersheds Swtr 01, Swtr 02, and Swtr 04 recorded the highest values (>40 $m^3\ s^{-1}$), attributable to low vegetation and impervious areas. For instance, a Q_p of 65.25 $m^3\ s^{-1}$ was recorded in Swtr 02, closely related to the establishment of cities and paved areas, where runoff is due to low or nonexistent infiltration [77]. Several authors have used SWAT to simulate the hydrological response to historical rainfall records at the watershed scale. Besalatpour et al. [80] identified priority areas based on runoff, Tripathi et al. [24] prioritized areas with soil degradation issues to implement best management practices, and Phomcha et al. [81] employed SWAT to identify areas affected by erosion and recommended soil conservation actions at the sub-watershed level. These studies illustrate that SWAT is a powerful tool for determining variables directly related to degradation processes. In this study, the results for the hydrology criterion coincide with those of Tripathi et al. [24], as the main issues related to soil degradation in the watershed were associated with urban areas and grasslands.

Regarding hillslope stability and soil water saturation criteria, Swtr 07 and Swtr 08, located in the highlands, were classified as the sub-watersheds with the largest unstable area (*I*), of 501.45 ha and 657.44 ha, respectively. Most of each watershed has a soil water saturation index classified as wet (*H*), with 136.29 km^2 (42.69%), followed by dry (*Se*), with 121.94 km^2 (38.19%), and saturated zone (*Sa*), with 61.04 km^2 (19.12%). The areas with the highest soil water saturation are located near streams in the watershed lowlands. However, the sub-watersheds in the highlands (Swtr 05, Swtr 06, Swtr 07, and Swtr 08) have a greater influence on soil water saturation when combined with high-intensity rains, eroded soils, degraded land use, and areas susceptible to landslides. Due to the relief, runoff and sediment transport are more significant in the highlands, mainly because there are no large, saturated areas on the slopes. This combination causes hillslope instability due to an increase in soil water content, which reduces shear stress and triggers landslides [57,82,83]. Additionally, runoff and sediment deposition increase in the lowlands due to the decreasing slope and slower flow.

Regarding the land-use criterion, the most significant changes were recorded in Swtr 08 and Swtr 07, with reductions in high vegetation (*VA*) of 771.12 ha and 1174.59 ha, respectively, and increases in medium vegetation (*VM*) of 970.92 ha and 603.45 ha, respectively.

Consequently, the entire watershed experienced an average annual loss rate of high vegetation of 146 ha year^{-1}. The use of *NDVI* to prioritize drainage areas based on changes in land use and their relationship with watershed degradation has been successfully implemented in previous studies [84–86].

As for the socioeconomic conditions criterion, the Swtr 01, Swtr 02, and Swtr 03 are home to the most developed cities that provide basic services (electricity, drinking water, sewer systems); although, according to the marginalization index, the quality of life ranges from medium to low [63]. Swtr 08 comprises several communities with poor quality of life, and some basic services are not available [87]. In Swtr 06, the number of inhabitants is associated with coffee plantations in the area. The living conditions also have limitations; however, farm owners provide the most basic services and jobs on the farms [88]. In the highland sub-watersheds, population centers are located in areas susceptible to landslides [26]. In addition, changes in land use in these areas increase the risk of disasters since they occur along with a steep relief [30].

Finally, the ANP model allowed the identification of the criteria that had the greatest influence on the HRB degradation process. The most significant criteria are hydrology and land-use change. The former refers to the hydrological characteristics of sub-watersheds, which are closely related to rainfall conditions. Intense, short-duration rainfall events reaching up to 550 mm usually occur during the wettest month (September), leading to concentrated runoff along sub-watershed channels [88]. The latter regards variations in land use over time, leading to increased degradation, loss of soil fertility, and appearance of gullies due to water erosion [89]. These add to the poor management of natural resources and deforestation by the local inhabitants, mainly in highland sub-watersheds [28]. The differences in the behavior of the criteria in each sub-watershed set the foundations for the development of detailed management plans based on the actual watershed status. Thus, the results from the sub-criteria highlight the need to consider soil and water conservation activities, environmental ecology, and sustainable development [90].

Esc was the top priority of the sub-criteria evaluated, mainly related to intense rainfall events in the HRB. It causes soil detachment and sediment transport from the highlands and their deposition in the lowlands of the watershed [26,91]. The socioeconomic criterion was the lowest priority [92], although its importance lies in knowing the interaction between the environment and the local inhabitants of the watershed [65]. Therefore, proposals to mitigate degradation in priority areas should focus on hydrology and land-use change criteria, implementing projects with particular emphasis on controlling surface runoff and reducing forest loss due to changes in land use.

5. Conclusions

The ANP model was highly effective in prioritizing sub-watersheds in the Huehuetan River Basin (HRB), allowing a nuanced assessment of degradation based on criteria such as morphometry, hydrology, slope stability, soil saturation, land use change, and socioeconomic factors. Hydrology (20.62%) and land-use change (19.82%) were the primary drivers of prioritization, highlighting the impact of high surface runoff and deforestation, respectively. Consequently, sub-watersheds Swtr 08 and Swtr 07, both in the upper basin, were designated as the top priorities, covering 24.31% of the HRB. In particular, 55.31% of the area in Swtr 08 was considered unstable; together, these sub-watersheds have experienced a high-vegetation loss totaling 16.46 km^2.

To address these vulnerabilities, targeted interventions are essential, including sediment flow controls, soil restoration, and forest conservation to mitigate degradation and stabilize soil. The methodology used provides a scalable and adaptable model for similar watersheds, accommodating various natural, socioeconomic, and cultural contexts. It offers a robust framework for identifying high-risk areas and guiding effective integrated watershed management plans to optimize resource allocation and mitigate environmental impact.

Supplementary Materials: The following supporting information can be downloaded at: https://www.mdpi.com/article/10.3390/land13111868/s1, Table S1. Values of sub-criteria with the highest influence in each sub-watershed, Table S2. Unweighted supermatrix, Table S3. Weighted Supermatrix and Table S4. Limit Supermatrix.

Author Contributions: Conceptualization, A.L.-P. and G.C.-G.; methodology, A.L.-P., M.A.B.-G. and D.S.F.-R.; software, A.L.-P., G.C.-G. and H.M.; validation, A.L.-P. and G.C.-G.; formal analysis, A.L.-P., G.C.-G. and H.M.; investigation, A.L.-P.; writing—original draft preparation, A.L.-P., G.C.-G., H.M. and A.S.C.-R.; writing—review and editing, A.L.-P., G.C.-G., H.M., M.A.B.-G., D.S.F.-R. and A.S.C.-R. All authors have read and agreed to the published version of the manuscript.

Funding: This study was financed by the Consejo Nacional de Humanidades, Ciencias y Tecnologías (CONAHCYT), for funding the Ph.D. studies of A.L.P. (CVU. 175394). Hector Moya was funded by the Agencia Nacional de Investigación y Desarrollo (ANID) in the Centro Regional de Investigación e Innovación para la Sostenibilidad de la Agricultura y los Territorios Rurales (CERES) (R23F0003), Pontificia Universidad Católica de Valparaíso (PUCV).

Data Availability Statement: The data supporting the findings of this study are available from the corresponding author upon reasonable request.

Conflicts of Interest: The authors declare no conflicts of interest.

References

1. Alilou, H.; Rahmati, O.; Singh, V.P.; Choubin, B.; Pradhan, B.; Keesstra, S.; Ghiasi, S.S.; Sadeghi, S.H. Evaluation of Watershed Health Using Fuzzy-ANP Approach Considering Geo-Environmental and Topo-Hydrological Criteria. *J. Environ. Manag.* **2019**, *232*, 22–36. [CrossRef] [PubMed]
2. Wang, G.; Mang, S.; Cai, H.; Liu, S.; Zhang, Z.; Wang, L.; Innes, J.L. Integrated Watershed Management: Evolution, Development and Emerging Trends. *J. For. Res.* **2016**, *27*, 967–994. [CrossRef]
3. Gajbhiye, S.; Mishra, S.K.; Pandey, A. Prioritizing Erosion-Prone Area through Morphometric Analysis: An RS and GIS Perspective. *Appl. Water Sci.* **2013**, *4*, 51–61. [CrossRef]
4. Trabucchi, M.; Comín, F.A.; O'Farrell, P.J. Hierarchical Priority Setting for Restoration in a Watershed in NE Spain, Based on Assessments of Soil Erosion and Ecosystem Services. *Reg. Environ. Chang.* **2013**, *13*, 911–926. [CrossRef]
5. Halder, S.; RoyChowdhury, A.; Kar, S.; Ray, D.; Bhandari, G. Critical Watershed Prioritization through Multi-Criteria Decision-Making Techniques and Geographical Information System Integration for Watershed Management. *Sustainability* **2024**, *16*, 3467. [CrossRef]
6. Wang, B.; Song, J.; Ren, J.; Li, K.; Duan, H.; Wang, X. Selecting Sustainable Energy Conversion Technologies for Agricultural Residues: A Fuzzy AHP-VIKOR Based Prioritization from Life Cycle Perspective. *Resour. Conserv. Recycl.* **2019**, *142*, 78–87. [CrossRef]
7. Shahraki, A.R.; Paghaleh, M.J. Ranking the Voice of Customer with Fuzzy DEMATEL and Fuzzy AHP. *Indian J. Sci. Technol.* **2011**, *4*, 1763–1772. [CrossRef]
8. Tellaeche, A.; BurgosArtizzu, X.P.; Pajares, G.; Ribeiro, A.; Fernández-Quintanilla, C. A New Vision-Based Approach to Differential Spraying in Precision Agriculture. *Comput. Electron. Agric.* **2008**, *60*, 144–155. [CrossRef]
9. Qin, X.S.; Huang, G.H.; Chakma, A.; Nie, X.H.; Lin, Q.G. A MCDM-Based Expert System for Climate-Change Impact Assessment and Adaptation Planning—A Case Study for the Georgia Basin, Canada. *Expert Syst. Appl.* **2008**, *34*, 2164–2179. [CrossRef]
10. Simonovic, S.P.; Verma, R. A New Methodology for Water Resources Multicriteria Decision Making under Uncertainty. *Phys. Chem. Earth Parts A/B/C* **2008**, *33*, 322–329. [CrossRef]
11. Vulević, T.; Dragović, N. Multi-Criteria Decision Analysis for Sub-Watersheds Ranking via the PROMETHEE Method. *Int. Soil Water Conserv. Res.* **2017**, *5*, 50–55. [CrossRef]
12. Bohra, B.M.; Bhardwaj, A. Watershed Prioritization of Upper Kosi Watershed Based on Soil Erodibility Computed through TanDEM-X DEM and TOPSIS-AHP Ensemble Model. In Proceedings of the 1st International Electronic Conference on Applied Sciences, Online, 10–30 November 2020.
13. dos Anjos Luís, A.; Cabral, P. Small Dams/Reservoirs Site Location Analysis in a Semi-Arid Region of Mozambique. *Int. Soil Water Conserv. Res.* **2021**, *9*, 381–393. [CrossRef]
14. Alanís-Anaya, R.M.; Legorreta-Paulín, G.; Mas, J.F.; Granados-Ramírez, G.R. Susceptibility to Gravitational Processes Due to Land Cover Change in the Río Chiquito-Barranca Del Muerto Subbasin (Pico De Orizaba Volcano, México). *J. Mt. Sci.* **2017**, *14*, 2511–2526. [CrossRef]
15. Nekhay, O.; Arriaza, M.; Boerboom, L. Evaluation of Soil Erosion Risk Using Analytic Network Process and GIS: A Case Study from Spanish Mountain Olive Plantations. *J. Environ. Manag.* **2009**, *90*, 3091–3104. [CrossRef] [PubMed]
16. Patel, A.; Singh, M.M.; Singh, S.K.; Kushwaha, K.; Singh, R. AHP and TOPSIS Based Sub-Watershed Prioritization and Tectonic Analysis of Ami River Basin, Uttar Pradesh. *J. Geol. Soc. India* **2022**, *98*, 423–3430. [CrossRef]

17. Borji, M.; Samani, A.N.; Rashidi, S.; Tiefenbacher, J.P. Catchment-Scale Soil Conservation: Using Climate, Vegetation, and Topo-Hydrological Parameters to Support Decision Making and Implementation. *Sci. Total Environ.* **2020**, *712*, 136124. [CrossRef]
18. Tzeng, G.H.; Huang, C.Y. Combined DEMATEL Technique with Hybrid MCDM Methods for Creating the Aspired Intelligent Global Manufacturing & Logistics Systems. *Ann. Oper. Res.* **2012**, *197*, 159–190. [CrossRef]
19. Adhami, M.; Sadeghi, S.H. Sub-Watershed Prioritization Based on Sediment Yield Using Game Theory. *J. Hydrol.* **2016**, *541*, 977–987. [CrossRef]
20. Chen, Y.; Jin, Q.; Fang, H.; Lei, H.; Hu, J.; Wu, Y.; Chen, J.; Wang, C.; Wan, Y. Analytic Network Process: Academic Insights and Perspectives Analysis. *J. Clean. Prod.* **2019**, *235*, 1276–1294. [CrossRef]
21. Teshome, A.; de Graaff, J.; Stroosnijder, L. Evaluation of Soil and Water Conservation Practices in the North-Western Ethiopian Highlands Using Multi-Criteria Analysis. *Front. Environ. Sci.* **2014**, *2*, 112382. [CrossRef]
22. Ebrahimi Gatgash, Z.; Sadeghi, S.H. Prioritization-Based Management of the Watershed Using Health Assessment Analysis at Sub-Watershed Scale. *Environ. Dev. Sustain.* **2023**, *25*, 9673–9702. [CrossRef]
23. Yadav, S.K.; Dubey, A.; Szilard, S.; Singh, S.K. Prioritisation of Sub-Watersheds Based on Earth Observation Data of Agricultural Dominated Northern River Basin of India. *Geocarto Int.* **2018**, *33*, 339–356. [CrossRef]
24. Tripathi, M.P.; Panda, R.K.; Raghuwanshi, N.S. Identification and Prioritisation of Critical Sub-Watersheds for Soil Conservation Management Using the SWAT Model. *Biosyst. Eng.* **2003**, *85*, 365–379. [CrossRef]
25. Meshram, S.G.; Alvandi, E.; Meshram, C.; Kahya, E.; Fadhil Al-Quraishi, A.M. Application of SAW and TOPSIS in Prioritizing Watersheds. *Water Resour. Manag.* **2020**, *34*, 715–732. [CrossRef]
26. Arellano-Monterrosas, J.L.L. Integrated Water Resources Management to Reduce the Vulnerability to Land Sliding and Flooding in the Sierra Madre of Chiapas Watersheds. *Ing. Agríc. Biosist.* **2010**, *2*, 23–37. [CrossRef]
27. Andrade-Velázquez, M.; Medrano-Pérez, O.R. Patrones de Precipitación En Las Cuencas Usumacinta y Grijalva (Sur de México) Bajo Un Clima Cambiante. *Rev. Bio Cienc.* **2020**, *7*, 1–22. [CrossRef]
28. Escobar Flores, R.E.; Castillo Santiago, M.Á.; Escobar Flores, R.E.; Castillo Santiago, M.Á. Land Cover and Land Use Change in the Soconusco Region, State of Chiapas. *Rev. Mex. Cienc. For.* **2021**, *12*, 46–69. [CrossRef]
29. Murcia, H.F.; Macías, J.L. Registro geológico de inundaciones recurrentes e inundación del 4 de octubre de 2005 en la ciudad de Tapachula, Chiapas, México. *Rev. Mex. Cienc. Geol.* **2009**, *26*, 1–17.
30. Arellano-Monterrosas, J.L. *Vulnerabilidad y Gestión de Riesgos Por Deslizamientos e Inundaciones En La Cuenca Superior Del Río Huehuetán, Chiapas*; Instituto Mexicano de Tecnología del Agua: Jiutepec, Mexico, 2012.
31. Verdin, K.L.; Verdin, J.P. A Topological System for Delineation and Codification of the Earth's River Basins. *J. Hydrol.* **1999**, *218*, 1–12. [CrossRef]
32. INEGI Continuo de Elevaciones Mexicano (CEM) 3.0. Available online: https://www.inegi.org.mx/app/geo2/elevacionesmex/ (accessed on 1 February 2018).
33. García, E. *Modificaciones al Sistema de Clasificación Climática de Koppen: Para Adaptarlo a Las Condiciones de La República Mexicana; Quinta*; Instituto de Geografía-UNAM: México, Mexico, 2004.
34. INEGI Climas 1902–2011. Available online: https://www.inegi.org.mx/app/biblioteca/ficha.html?upc=889463769361 (accessed on 9 October 2024).
35. INEGI Red Hidrográfica. Escala 1:50,000. Edición 2.0. Subcuenca Hidrográfica RH23Ag R. Huehuetán. Cuenca R. Suchiate y Otros. RH Costa de Chiapas. Available online: https://www.inegi.org.mx/app/biblioteca/ficha.html?upc=889463127086 (accessed on 31 March 2024).
36. INEGI Conjunto de Datos Edafológicos. Escala 1:1,000,000 Serie I. Available online: https://www.inegi.org.mx/app/biblioteca/ficha.html?upc=702825267636 (accessed on 30 April 2023).
37. Horton, R.E. Drainage-Basin Characteristics. *Eos Trans. Am. Geophys. Union* **1932**, *13*, 350–361. [CrossRef]
38. Strahler, A.N. Quantitative Analysis of Watershed Geomorphology. *Eos Trans. Am. Geophys. Union* **1957**, *38*, 913–920. [CrossRef]
39. Strahler, A.N. Hypsometric (Area-Altitude) Analysis of Erosional Topography. *Geol. Soc. Am. Bull.* **1952**, *63*, 1117–1142. [CrossRef]
40. Pérez-Peña, J.V.; Azañón, J.M.; Azor, A. CalHypso: An ArcGIS Extension to Calculate Hypsometric Curves and Their Statistical Moments. Applications to Drainage Basin Analysis in SE Spain. *Comput. Geosci.* **2009**, *35*, 1214–1223. [CrossRef]
41. Odiji, C.A.; Aderoju, O.M.; Eta, J.B.; Shehu, I.; Mai-Bukar, A.; Onuoha, H. Morphometric Analysis and Prioritization of Upper Benue River Watershed, Northern Nigeria. *Appl. Water Sci.* **2021**, *11*, 41. [CrossRef]
42. Arnold, J.G.; Srinivasan, R.; Muttiah, R.S.; Williams, J.R. Large area hydrologic modeling and assessment part I: Model development. *JAWRA J. Am. Water Resour. Assoc.* **1998**, *34*, 73–89. [CrossRef]
43. Dile, Y.T.; Daggupati, P.; George, C.; Srinivasan, R.; Arnold, J. Introducing a New Open Source GIS User Interface for the SWAT Model. *Environ. Model. Softw.* **2016**, *85*, 129–138. [CrossRef]
44. Arnold, J.G.; Moriasi, D.N.; Gassman, P.W.; Abbaspour, K.C.; White, M.J.; Srinivasan, R.; Santhi, C.; Harmel, R.D.; van Griensven, A.; Van Liew, M.W.; et al. SWAT: Model Use, Calibration, and Validation. *Trans. ASABE* **2012**, *55*, 1491–1508. [CrossRef]
45. Velescu, A. *Heterogenität von Bodenkundlichen Standortfaktoren in Feucht-Tropischen Gebirgslandschaften Am Beispiel Des Einzungsgebietes Des Río Huehuetán (Chiapas, Mexiko)*; Diplomarbeit, Eberhard-Karls-Universität Tübingen: Tübingen, Germany, 2009.
46. Guijarro, J.A. *Homogenization of Climatic Series with Climatol*; Reporte técnico State Meteorological Agency (AEMET), Balearic Islands Office: Baleares, Spain, 2018.

47. Fuka, D.R.; Walter, M.T.; Macalister, C.; Degaetano, A.T.; Steenhuis, T.S.; Easton, Z.M. Using the Climate Forecast System Reanalysis as Weather Input Data for Watershed Models. *Hydrol. Process.* **2014**, *28*, 5613–5623. [CrossRef]
48. Chen, C. Rainfall Intensity-Duration-Frequency Formulas. *J. Hydraul. Eng.* **1983**, *109*, 1603–1621. [CrossRef]
49. Campos-Aranda, D.F. *Estimación y Aprovechamiento Del Escurrimiento*; UNAM, Instituto de Ingeniería: Ciudad de México, Mexico, 2007; ISBN 9789709511802.
50. Arteaga Ramírez, R.; Aguirre Rodríguez, A.; Sangerman-Jarquín, D.M.; Vázquez Peña, M.A.; Ibáñez Castillo, L.A.; Hernández Mendoza, T.M. Presión de Vapor Actual Observada y Estimada En Observatorios Sinópticos de México. *Rev. Mex. Cienc. Agric.* **2010**, *1*, 77–87.
51. CONAGUA Sistema de Información Hidrológica (SIH). Available online: https://sih.conagua.gob.mx/ (accessed on 8 August 2024).
52. Pinto, D.B.F.; Da Silva, A.M.; De Mello, C.R.; Beskow, S.; Coelho, G. Application of the Soil and Water Assessment Tool (SWAT) for Sediment Transport Simulation at a Headwater Watershed in Minas Gerais State, Brazil. *Trans. ASABE* **2013**, *56*, 697–709. [CrossRef]
53. Rivas-Tabares, D.; de Miguel, Á.; Willaarts, B.; Tarquis, A.M. Self-Organizing Map of Soil Properties in the Context of Hydrological Modeling. *Appl. Math. Model.* **2020**, *88*, 175–189. [CrossRef]
54. Moriasi, D.N.; Gitau, M.W.; Pai, N.; Daggupati, P. Hydrologic and Water Quality Models: Performance Measures and Evaluation Criteria. *Trans. ASABE* **2015**, *58*, 1763–1785. [CrossRef]
55. Pack, R.T.; Tarboton, D.G.; Goodwin, C.N. The SINMAP Approach to Terrain Stability Mapping. In Proceedings of the 8th Congress of the International Association of Engineering Geology, Vancouver, BC, Canada, 21–25 September 1998.
56. Tarolli, P.; Tarboton, D.G. A New Method for Determination of Most Likely Landslide Initiation Points and the Evaluation of Digital Terrain Model Scale in Terrain Stability Mapping. *Hydrol. Earth Syst. Sci.* **2006**, *10*, 663–677. [CrossRef]
57. Michel, G.P.; Kobiyama, M.; Goerl, R.F. Comparative Analysis of SHALSTAB and SINMAP for Landslide Susceptibility Mapping in the Cunha River Basin, Southern Brazil. *J. Soils Sediments* **2014**, *14*, 1266–1277. [CrossRef]
58. Pradhan, A.M.S.; Kim, Y.T. Application and Comparison of Shallow Landslide Susceptibility Models in Weathered Granite Soil under Extreme Rainfall Events. *Environ. Earth Sci.* **2015**, *73*, 5761–5771. [CrossRef]
59. Swets, J.A. Measuring the Accuracy of Diagnostic Systems. *Science 1979* **1988**, *240*, 1285–1293. [CrossRef]
60. Hosmer, D.W.; Lemeshow, S. Assessing the Fit of the Model. In *Applied Logistic Regression*; Wiley: Hoboken, NJ, USA, 2000; pp. 143–202. [CrossRef]
61. Merg, C.; Petri, D.; Bodoira, F.; Nini, M.; Díez, M.J.F.; Schmindt, F.; Montalva, R.; Guzmán, L.; Rodríguez, K.; Blanco, F. Mapas Digitales Regionales de Lluvias, Índice Estandarizado de Precipitación e Índice Verde. *Pilquen-Sección Agron.* **2011**, *5*, 1–11.
62. Hayes, L. Review Article The Current Use of TIROS-N Series of Meteorological Satellites for Land-Cover Studies. *Int. J. Remote Sens.* **1985**, *6*, 35–45. [CrossRef]
63. CONEVAL. *Informe de Pobreza y Evaluación 2020*; Consejo Nacional de Evaluación de la Política de Desarrollo Social: Ciudad de México, Mexico, 2020.
64. CentroGeo Metadatos de: Localidades de México, INEGI. 2010. Available online: https://idegeo.centrogeo.org.mx/layers/geonode:unikloc10gw/layer_info_metadata (accessed on 29 February 2016).
65. Soares, D.; Peña, A. Vulnerabilidad Frente a Huracanes Desde La Perspectiva de Los Actores Sociales Locales. *Soc. Ambiente* **2014**, *1*, 48–72. [CrossRef]
66. Tzeng, G.-H.; Huang, J.-J. Analytic Network Process and Fuzzy Analytic Network Process. In *Multiple Attribute Decision Making*; Taylor & Francis Group: Abingdon, UK, 2011; pp. 43–68. [CrossRef]
67. Gómez-Navarro, T.; García-Melón, M.; Acuña-Dutra, S.; Díaz-Martín, D. An Environmental Pressure Index Proposal for Urban Development Planning Based on the Analytic Network Process. *Environ. Impact Assess. Rev.* **2009**, *29*, 319–329. [CrossRef]
68. Saaty, T.L. Decision Making—The Analytic Hierarchy and Network Processes (AHP/ANP). *J. Syst. Sci. Syst. Eng.* **2004**, *13*, 1–35. [CrossRef]
69. Khanday, M.Y.; Javed, A. Hydrological Investigations in the Semi-Arid Makhawan Watershed, Using Morphometry. *Appl. Water Sci.* **2017**, *7*, 3919–3936. [CrossRef]
70. Ishizaka, A.; Labib, A. Review of the Main Developments in the Analytic Hierarchy Process. *Expert Syst. Appl.* **2011**, *38*, 14336–14345. [CrossRef]
71. RazaviToosi, S.L.; Samani, J.M.V. Evaluating Water Management Strategies in Watersheds by New Hybrid Fuzzy Analytical Network Process (FANP) Methods. *J. Hydrol.* **2016**, *534*, 364–376. [CrossRef]
72. Giner-Santonja, G.; Aragonés-Beltrán, P.; Niclós-Ferragut, J. The Application of the Analytic Network Process to the Assessment of Best Available Techniques. *J. Clean. Prod.* **2012**, *25*, 86–95. [CrossRef]
73. Calizaya, A.; Meixner, O.; Bengtsson, L.; Berndtsson, R. Multi-Criteria Decision Analysis (MCDA) for Integrated Water Resources Management (IWRM) in the Lake Poopo Basin, Bolivia. *Water Resour. Manag.* **2010**, *24*, 2267–2289. [CrossRef]
74. Bharath, A.; Kumar, K.K.; Maddamsetty, R.; Manjunatha, M.; Tangadagi, R.B.; Preethi, S. Drainage Morphometry Based Sub-Watershed Prioritization of Kalinadi Basin Using Geospatial Technology. *Environ. Chall.* **2021**, *5*, 100277. [CrossRef]
75. Guns, M.; Vanacker, V. Forest Cover Change Trajectories and Their Impact on Landslide Occurrence in the Tropical Andes. *Environ. Earth Sci.* **2013**, *70*, 2941–2952. [CrossRef]
76. Collins, B.D.; Znidarcic, D. Closure to "Stability Analyses of Rainfall-Induced Landslides" by Brian D. Collins and Dobroslav Znidarcic. *J. Geotech. Geoenviron. Eng.* **2005**, *131*, 1438. [CrossRef]

77. Ruiz Meza, L.E. Género y Percepciones Sociales Del Riesgo y La Variabilidad Climática En La Región Del Soconusco, Chiapas. *Alteridades* **2014**, *24*, 77–88.
78. Cătalin Dobrea, R.; Molănescu, G.; Buşu, C.; Vasile, A.J.; Gheorghe, P. Food Sustainable Model Development: An ANP Approach to Prioritize Sustainable Factors in the Romanian Natural Soft Drinks Industry Context. *Sustainability* **2015**, *7*, 10007–10020. [CrossRef]
79. Nautiyal, M.D. Morphometric Analysis of a Drainage Basin Using Aerial Photographs: A Case Study of Khairkuli Basin, District Dehradun, U.P. *J. Indian Soc. Remote Sens.* **1994**, *22*, 251–261. [CrossRef]
80. Besalatpour, A.; Hajabbasi, M.A.; Ayoubi, S.; Jalalian, A. Identification and Prioritization of Critical Sub-Basins in a Highly Mountainous Watershed Using SWAT Model. *Eurasian J. Soil Sci.* **2012**, *1*, 58–64.
81. Phomcha, P.; Wirojanagud, P.; Vangpaisal, T.; Thaveevouthti, T. Modeling the Impacts of Alternative Soil Conservation Practices for an Agricultural Watershed with the SWAT Model. *Procedia Eng.* **2012**, *32*, 1205–1213. [CrossRef]
82. Ma, S.; Shao, X.; Xu, C. Landslides Triggered by the 2016 Heavy Rainfall Event in Sanming, Fujian Province: Distribution Pattern Analysis and Spatio-Temporal Susceptibility Assessment. *Remote Sens.* **2023**, *15*, 2738. [CrossRef]
83. Aristizábal, P.E.; Martínez, H.; Vélez, J.I. Una revisión sobre el estudio de movimientos en masa detonados por lluvias. *Rev. Acad. Colomb. Cienc. Exactas Fis. Nat.* **2010**, *34*, 209–227. [CrossRef]
84. Nyamekye, C.; Osei Jnr, E.M.; Oseitutu, A. Classification of Time Series NDVI for the Assessment of Land Cover Change in Ghana Using NOAA/AVHRR Data. *J. Geomat.* **2014**, *8*, 34–39.
85. El-Gammal, M.I.; Ali, R.R.; Samra, R.A. NDVI Threshold Classification for Detecting Vegetation Cover in Damietta Governorate, Egypt. *J. Am. Sci.* **2014**, *10*, 108–113.
86. Jomaa, I.; Bou Kheir, R.; Gitas, I.Z.; San Miguel Ayanz, J. Multitemporal Unsupervised Classification and NDVI to Monitor Land Cover Change in Lebanon (1987–1998). *Options Méditerranéennes Série B Etudes Et Rech.* **2003**, *46*, 43–49.
87. Ruiz, L.E.; Arellano, J.L. *Identificación Comunitaria de Riesgos Climáticos, Medios de Vida y Estrategias de Adaptación En La Cuenca Del Río Huhuetán, En Chiapas. Reflexiones y Expresiones de La Vulnerabilidad Social en el Sureste de México*; IIMTA: Cuernavaca, Mexico, 2014; pp. 79–121.
88. Ayala-Carrillo, M.d.R.; Zapata-Martelo, E.; Suárez-San Román, B.; Nazar-Beautelspacher, A. Estrategias de Reproducción Familiar En Las Fincas Cafetaleras Del Soconusco, Chiapas. *Agric. Soc. Desarro.* **2014**, *11*, 401–423. [CrossRef]
89. Pérez-Nieto, S.; Arellano-Monterrosas, J.L.; Ibáñez-Castillo, L.A.; Hernández-Saucedo, F.R. Estimación de La Erosión Hídrica Provocada Por El Huracán Stan En Las Cuencas Costeras de Chiapas, México. *Rev. Terra Latinoam.* **2012**, *30*, 103–110.
90. Tesema, T.A. Impact of Identical Digital Elevation Model Resolution and Sources on Morphometric Parameters of Tena Watershed, Ethiopia. *Heliyon* **2021**, *7*, e08345. [CrossRef] [PubMed]
91. Baumann, J.; Arrellano-Monterrosas, J.L.; Borgman, J. Adaptation of the Universal Soil Loss Equation to the Tropical Pacific Coastal Region of the Chiapas State, Mexico. In Proceedings of the 12th ISCO Conference—12th International Soil Conservation, Beijing, China, 31 May 2002; pp. 518–523.
92. Al-Ruzouq, R.; Shanableh, A.; Yilmaz, A.G.; Idris, A.E.; Mukherjee, S.; Khalil, M.A.; Gibril, M.B.A. Dam Site Suitability Mapping and Analysis Using an Integrated GIS and Machine Learning Approach. *Water* **2019**, *11*, 1880. [CrossRef]

Disclaimer/Publisher's Note: The statements, opinions and data contained in all publications are solely those of the individual author(s) and contributor(s) and not of MDPI and/or the editor(s). MDPI and/or the editor(s) disclaim responsibility for any injury to people or property resulting from any ideas, methods, instructions or products referred to in the content.